INDUSTRIAL HEAT EXCHANGERS EVALUATION USING THERMAL DESIGN AND OPTIMIZATION

JUAN SEBASTIÁN RINCÓN TABARES

UNIVERSIDAD AUTÓNOMA DE MANIZALES
FACULTAD DE INGENIERÍA
MAESTRÍA EN INGENIERÍA
MANIZALES
2018

INDUSTRIAL HEAT EXCHANGERS EVALUATION USING THERMAL DESIGN AND OPTIMIZATION.

JUAN SEBASTIÁN RINCÓN TABARES

Proyecto de grado para optar al título de Magíster en Ingeniería

Tutor:

MSC. LUIS PERDOMO HURTADO

Cotutor:

MSC. FABIO MARCELO PEÑA BUSTOS

UNIVERSIDAD AUTÓNOMA DE MANIZALES
FACULTAD DE INGENIERÍA
MAESTRÍA EN INGENIERÍA
MANIZALES
2018

DEDICATION

To my family for all their support.

ACKNOWLEDGEMENTS

I want to thank my research advisors Msc. Luis Perdomo Hurtado and Msc. Fabio Marcelo Peña Bustos for their exceptional guidance during my period in Universidad Autónoma de Manizales's Engineering Masters. Their support and constant encouragement during the course of this work was fundamental to reach my objectives.

Thanks to PhD. Jose Luis Aragón Vera director of Centro de Física Aplicada y Tecnología Avanzada of Universidad Nacional Autónoma de México who received and guided me during my research internship at the center in October of 2017.

Deep thanks to all members of Mecánica y Producción department from Universidad Autónoma de Manizales, especially to Prof. Alba Patricia Arias Orozco (Dean of Engineering Faculty), Prof. Alex Mauricio Ovalle Castiblanco (Head of Mecánica y Producción department), Prof. Sebastián Durango Idarraga and Prof. Cesar Augusto Álvarez Vargas due to their personal interest in the development of my research and academic processes.

Additionally, it is a pleasure to thank to members from UAM community: Eng. Carlos Eduardo Jaramillo Sanint (Director of financial Affairs), Dr. Iván Escobar Escobar (Director of Academic Affairs), Prof. Diana Yomali Ospina López (coordinator of Engineering Masters) and Prof. Francy Nelly Jiménez García (former coordinator of Engineering Masters) for their gracious and timely management at critical moments at the beginning and during the development of my master's degree.

Finally, I want to express my sincere gratitude to my parents Gloria Isabel Tabares Escobar and Argemiro Rincón Arango and my older siblings because they are pillars where I am building my life project.

ABSTRACT

This Engineering Master dissertation contributes to the energy efficiency area by applying "Thermal design and optimization" methodologies to evaluate industrial feasible heat exchangers via two case studies.

In a first approach, an enhancement to standard castor oil bio-diesel production process was proposed by adding an oil preheater in a place just before pumping the raw material to the transesterification process. A methodology to select this preheater was developed by comparing exergy transfer effectiveness and entropy generation in the usual fluid arrangements for heat exchangers. Due to the best Second Law performance, Shell-&-Tube arrangement was selected and some configurations analyzed by Bell-Delaware method to choose those geometric parameters that perform best. It is to highlight that configuration that has the standard manufacturing recommended geometry relations is in very good agreement with exergy and second law analysis.

On the other hand, Plate-&-Frame heat exchangers have their main application in food processing industry when a liquid - liquid situation is required. Due to this, 40 feasible gasketed-plate water-water heat exchangers were simulated to show their behavior, by a performance analysis, using First and Second Thermodynamic Laws indexes on some operational configurations of them. Operational variable parameters were heat exchanger area, cold fluid port connection allocation and room temperature. Main conclusion is that counter-current configurations have better performance than parallel flow configurations due to influence of finite temperature difference. Additionally, room temperature difference is a parameter that must be taken into account to select this kind of heat exchanger.

Keywords: Energy efficiency, indicators, thermal design and optimization, heat exchangers.

Table of Contents

List of Tables

List of Figures

1. INTRODUCTION

Energy efficiency, as well as the sustainable use of energy, have become priority issues due to the scarcity of non-renewable energy resources and the still insufficient capacity of renewable assets to cover global energy demand. In 2014, the gross world supply of energy was 13550.52 megaton equivalents of oil, of which only 13.3% was supplied by renewable sources, 5.6% by nuclear fission reactors and the rest by non-renewable sources [1]. This and other factors have precipitated the price of a barrel of crude until around $40 USD$ both the Brent and the WTI [2]. Meanwhile, the International Energy Agency projects that, by the year 2040, the energy consumption of the planet will be almost 50 % higher than that which currently exists. The aforementioned, added to almost 3 percentage points per year of growth in the economy, results in an economic behavior that would tend more and more to lower energy consumption with new policies of efficiency and rational use of this resource [2], [3].

Colombia is considered a country with a relatively good energy supply [4]. Here industry distributes its energy consumption as follows: 40% of natural gas, 24% electric power, 17% coal and mineral coke, 7% by oxidation of oil and its derivatives and the rest in unconventional alternative sources. Previous data represents the 22% of the nation's total energy demand. Even so, the import of gaseous fuel is expected to begin in the future. The data presented by Unidad de Planeación Minero-Energética in [5] may lead one to think that there are only two options for the country to remain independent in terms of energy: increasing production or decreasing consumption. The first path would be the simplest for consumers, however, there are limitations such as the search for new sources of energy, such as fuels, which must be inexpensive and have a low carbon footprint to meet these energy needs without significantly affecting society [6], [7]. On the other hand, the second option was not popular and was considered ineffective for developing countries, despite this, some publications show the contrary [8].Therefore, reasonable, sustain-

able and efficient use of energy seems to be a viable long-term solution for the economic-social condition of the countries.

Implementation of programs of energy efficient use in the industry, results in economic savings, lower costs of production, reduction of pollution and carbon footprint, in the productive chains. The advantages of an energy efficiency process are the reduction of current energy consumption, it does not produce pollution or generate a serious environmental impact. Among its results are the reduction of energy costs and increased competitiveness, reduction of greenhouse gases, creation of a culture of efficient use of resources and zero impact on food production. According to Quispe [9] for every 1 USD invested in efficiency to reduce 1 kWh, 4 USD is not invested in installing 1 kWh, it is a business with profitability between 10% and 17%, and even more important, it is the business where company assumes the least risks.

Wall, Ertesvåg and Mielnik in [10]–[12] show the close relationship that exists between sustainable processes with their second law or efficiency thermodynamic efficiency or exergy efficiency. This means that by improving the exergy efficiency (or minimizing the generation of entropy) in the processes, a lower energy consumption is ensured, less energy and materials are required and lost in the effluents, as well as a decrease in polluting emissions to environment [13]. "Thermal design and optimization" are methodologies for the projection of heat-based systems that emphasize economic engineering, process simulation and optimization techniques. Its thermodynamic formulation is based on exergy analysis, the minimization of entropy generation and thermo-economics[14].

The current work presents methodologies based on "Thermal design and optimization" to evaluate the performance of heat exchangers under feasible industrial conditions. To make it, secondary objectives were proposed. First, thermodynamic models for Shell-&-Tube heat exchangers and Plate-&-Frame heat exchangers were formulated; after that, entropy and exergy indicators were adapted to heat exchanger models; and, finally energy efficiency charts of Shell-&-Tube heat exchangers and Plate-&-Frame (also named Gasketed-Plate) heat exchangers were created to show some guidelines to evaluate the performance of the equipment. Those kinds of heat exchanger

were chosen, due to they are the two most commonly used types of heat exchanger on industry and are suitable for many applications [15], [16].

This dissertation collects two articles, produced during author current graduate course, for the same number of chapters. Each article, as the current section, is self-contained with sections adapted to the respective journal, but holding with the standard introduction, methods, results, and discussion scheme plus reference (bibliography) section. Some equations are repeated for the sake of clarity. After them, general concluding remarks are presented in chapter 4.

1.1. List of Publications

Table **1-1** presents the author current graduate course publications list. To avoid repetition and to respect the reader, paper drafts are presented in this document according to publisher copyright policies and self-archiving from SHERPA/RoMEO. For Energy Journal policy see [17] and for International Journal of Heat and Mass Transfer policy see [18].

Table 1-1: Summary of publications

	Title	State	Authors	Journal	Chapter
1.	Castor oil preheater selection based on entropy generation and exergy effectiveness criteria	Published	Luis Perdomo-Hurtado, Juan Sebastián Rincón Tabares, Danahe Marmolejo Correa, Felipe A. Perdomo	Energy, vol. 120, pp. 805–815, feb. 2017. ISSN: 0360-5442. See [19]	2
2.	Study of Gasketed-Plate Heat Exchanger performance based on energy efficiency indexes	Submited	Juan Sebastián Rincón Tabares, Jose Luis Aragón Vera, Luis Perdomo-Hurtado	International Journal of Heat and Mass Transfer (Elsevier), ISSN: 0017-9310	3

Bibliography

[1] Secretaria de Energia (SENER), *Balance nacional de energía 2014*, 2015.

[2] Unidad de Planeación Minero Energética, "Plan transitorio de abastecimiento de gas natural - versión noviembre 2016", Ministerio de Minas y Energía, Bogotá, Colombia, Dec. 5, 2016, p. 207. [Online]. Available: `http://www.upme.gov.co/SeccionHidrocarburos_sp/Publicaciones/2016/Plan_Transitorio_Abastecimiento_Gas_Natural.pdf` (visited on 02/26/2017).

[3] International Energy Agency, *World Energy Outlook 2016 Resumen Ejecutivo Spanish translation*, Español, Nov. 2016. (visited on 02/06/2017).

[4] Unidad de Planeación Minero Energética, *Integración de las energía renovables no convencionales en colombia*, 2015.

[5] ——, *Tendencias a largo plazo del sector energía en colombia*, 2014.

[6] Secretaria de Energia (SENER), *Programa Especial para el Aprovechamiento de Energias Renovables 2014 - 2018*. Mexico D.F.: Secretaria de Energia (SENER), 2014.

[7] ——, *Programa Nacional para el Aprovechamiento Sustentable de la Energia 2014 - 2018*. Mexico D.F., 2014, 57 pp. (visited on 07/13/2016).

[8] Casa Editorial El Tiempo. (Sep. 4, 2013). La eficiencia energética, cada vez con más luz en colombia, portafolio.co, [Online]. Available: `http://www.portafolio.co/negocios/empresas/eficiencia-energetica-vez-luz-colombia-82250` (visited on 07/22/2016).

[9] E. Quispe, "Eficiencia energética y competitividad empresarial oportunidades y desafíos", EXPO INDUSTRIAL: Feria de Soulciones Integrales para la Industria 2014, Centro de Eventos Valle del Pacífico, May 15, 2014, (visited on 07/05/2016).

[10] G. Wall, “EXERGY – a USEFUL CONCEPT”, PhD thesis, Chalmers University of Technology and University of Göteborg, Göteborg, Sweden, 1986, 38 pp.

[11] I. S. Ertesvåg and M. Mielnik, “Exergy analysis of the norwegian society”, *Energy*, vol. 25, no. 10, pp. 957–973, Oct. 2000, ISSN: 0360-5442. DOI: 10.1016/S0360-5442(00)00025-6. [Online]. Available: http://www.sciencedirect.com/science/article/pii/S0360544200000256 (visited on 07/13/2016).

[12] I. S. Ertesvåg, “Society exergy analysis: A comparison of different societies”, *Energy*, vol. 26, no. 3, pp. 253–270, Mar. 2001, ISSN: 0360-5442. DOI: 10.1016/S0360-5442(00)00070-0. [Online]. Available: http://www.sciencedirect.com/science/article/pii/S0360544200000700 (visited on 07/13/2016).

[13] M. G. Patterson, “What is energy efficiency?: Concepts, indicators and methodological issues”, *Energy Policy*, vol. 24, no. 5, pp. 377–390, 1996, ISSN: 0301-4215. [Online]. Available: http://econpapers.repec.org/article/eeeenepol/v_3a24_3ay_3a1996_3ai_3a5_3ap_3a377-390.htm (visited on 07/13/2016).

[14] A. Bejan, G. Tsatsaronis, and M. Moran, *Thermal Design and Optimization*, 1 edition. New York: Wiley-Interscience, Nov. 28, 1995, 560 pp., ISBN: 978-0-471-58467-4.

[15] S. Kakac, H. Liu, and A. Pramuanjaroenkij, *Heat exchangers: selection, rating, and thermal design*. CRC press, 2012, ISBN: 1-4398-4990-0.

[16] R. K. Shah and D. P. Sekulic, *Fundamentals of Heat Exchanger Design*. John Wiley & Sons, Aug. 11, 2003, 978 pp., ISBN: 978-0-471-32171-2.

[17] Centre for Research Communications - University of Nottingham. (). SHERPA/RoMEO - search - publisher copyright policies & self-archiving, Energy, [Online]. Available: http://www.sherpa.ac.uk/romeo/search.php?issn=0360-5442 (visited on 11/30/2018).

[18] ——, (). SHERPA/RoMEO - search - publisher copyright policies & self-archiving, International Journal of Heat and Mass Transfer, [Online]. Available: http://www.sherpa.ac.uk/romeo/search.php?issn=0017-9310 (visited on 11/30/2018).

[19] L. Perdomo-Hurtado, J. S. Rincón Tabares, D. Marmolejo Correa, and F. A. Perdomo, "Castor oil preheater selection based on entropy generation and exergy effectiveness criteria", *Energy*, vol. 120, pp. 805–815, Feb. 1, 2017, ISSN: 0360-5442. DOI: 10.1016/j.energy.2016.11.128. [Online]. Available: http://www.sciencedirect.com/science/article/pii/S0360544216317868 (visited on 02/22/2017).

2. CASTOR OIL PREHEATER SELECTION BASED ON MAXIMUM ENTROPY AND EXERGY EFFICIENCY CRITERIA

Luis Perdomo-Hurtado*, Juan Sebastián Rincón Tabares
*lperdomo@autonoma.edu.co
Departamento de Mecánica y producción, Universidad Autónoma de Manizales,
Antigua estación del ferrocarril, Manizales, Caldas, Colombia

Danahe Marmolejo Correa
Departamento de Ingeniería Física, División de Ciencias e ingeniería, Campus León,
Universidad de Guanajuato,
Loma del Bosque 103, Lomas del Campestre, 37150 León, Guanajuato, México

Felipe A. Perdomo
Programa de Ingeniería Química, Departamento de Ciencias Básicas e Ingeniería, Universidad de Bogotá Jorge Tadeo Lozano,
Cra 4 # 22 - 61 , Bogotá, Cundinamarca, Colombia

ABSTRACT

Castor oil has an especial hydroxyl fatty acid (cis-12-hydroxyoctadeca-9-enoic acid) which provides unique properties and unusual versatility as a raw material for biodiesel production. Major energy spending of biodiesel production is due to heating and pumping. Unless biodiesel industry can reduce the elevated energy demand, probably biodiesel will not be competitive and therefore this problem is more pronounced for castor oil biodiesel industry. In this work a preheater was

chosen in order to reduce pumping power by viscosity reduction and to reduce residence reactor time due to activation energy decreasing supply. The design procedure is based on exergy effectiveness transfer (EET) and maximum entropy (ME) approaches which are highly related with energy efficiency. A 2-1 shell-and-tube heat exchanger obtained the highest performance (in terms of EET and ME) among parallel, crossflow, counter current flow configurations here studied. Additionally, a thermodynamical model based on molecular theory ($SAFT-\gamma$) for castor oil was proposed to estimate thermodynamic properties that are required for the rigorous heat exchanger design, taking into account the eight most common fatty acid present in castor oil as a mixture.

2.1. Introduction

Biodiesel is considered as an alternative for diesel fuel obtained from vegetable oils or lipids with alcohol reactions. Biodiesel is nontoxic, biodegradable and environmentally friendly considered as a renewable energy sources that contributes to greenhouse gas reduction [1]. Biodiesel production mostly consists of a chemical reaction between vegetable or animal oil with alcohol such methanol. Conventional production processes refer to transesterification procedures which oils and alcohols react in liquid phase in the presence of a base catalyst (usually sodium hydroxide). These processes have a fatty acid feedstock at room temperature that is conduced to chemical reactor or a mixer (where it is blended with a methanol stream) by a pump.

There are different potential sources to obtain biodiesel such as fats and oils edible and non-edible, that can be used as raw material [2]. Castor oil, also known as Ricinus oil, is a fatty acid triglyceride (FA) within the seed of the castor plant, *Ricinus communis L.* Castor oil, rich in a very unique hydroxyl fatty acid (H-FA), ricinoleic acid $C_{18}H_{34}O_3$ structurally known as cis-12-hydroxyoctadeca-9-enoic acid, a 18 carbon hydroxylated fatty acid having one double bond. The presence of ricinoleic acid provides castor oil its unique properties and unusual versatility [3].Despite this, castor oil has the higher viscosity than other commercial fatty acid sources [4].

Biodiesel production from Ricinus oil has been identified as an important potential raw material for the local production of biodiesel in several places around the world and has become a

booming business [5], [6]. Castor oil biodiesel is lower cost in comparison to vegetable oils [1]. Nevertheless, high viscosity of the methyl ester from ricinoleic acid, exceeds the maximum value for kinematic viscosity in both ASTM D6751 and EN14214 biodiesel standards [7]. In addition, ricinoleic acid has higher viscosity than it produced methyl ester.

Biodiesel production has different kind of troubles. Despite efforts to reduce energy costs, they are still high (around 0.53 USD per liter [8]). Energy consumption is one of the most important challenge for biodiesel industry [9]. Unless biodiesel industry can reduce the elevated energy demand, probably biodiesel will not be competitive and therefore this problem is more pronounced for castor oil biodiesel industry. In order to reduce energy costs, preheated castor oil steam that enters to the chemical reactor could help to decrease energy costs due to fluid pumping power is generally elevated because of vegetable oils have high viscosities; so temperature increasing would reduce dynamic viscosity of vegetable oil.

On the other hand, higher conversion could be achieved by increasing the reaction temperature and reaction time, so if temperature gradient in the reactive mixture could be reduce then there is a direct reduction of heat that have to be added in the reactor [10]. For industrial biodiesel processes, there are different ways to design a biodiesel production process independent of its raw materials [11]. West et.al [12] have designed four processes to convert a waste vegetable oil feedstock into biodiesel, in which they work with a heat exchanger using the bottom distillation column to pre-heat their raw materials. The first two processes use pre-treated alkali and acid catalysts; the others employed a heterogeneous acid catalyst and a supercritical method.In order to aid energy costs in castor oil biodiesel production process, a preheater could reduce viscosity and pump load before to be taken to the reactor. In order to design a preheater, any heat exchanger design methodology requires not only thermodynamical properties of hot and cold fluids, as well as, dynamical properties for global heat transfer coefficient calculation and heat exchanger geometrical parameters [13].

Thermodynamical properties prediction for castor oil are limited a group contribution empirical models where a big amount of data for fatty acids like-molecules is fitted and extended for other

similar molecules [14]–[16]. Huber et.al [17] have developed an equation of state (EoS) for soy bean biodiesel using experimental data and thermodynamical theory. Molecular theories for FAs and theirs fatty acid methyl steres (FAMES) have been studied by Olivera et.al [18] comparing predictions between common cubic EoS and associating cubic EoS. Perdomo et.al [19] have developed a thermodynamical model for any FA, FAME and fatty acid ethyl ester (FAEE) and their mixtures based on the modification of the statistical association fluid theory called $SAFT-\gamma$ [20], [21]. This approach is used in this work in order to predict the thermophysical properties of Castor oil required in heat exchanger design methods.

Thermal analysis and design methods have been widely used for the study of thermal systems emphasizing engineering economics, system simulation, and optimization methods [22]. The methods of exergy analysis, entropy generation minimization, and thermoeconomics are the most used strategies to design thermal equipments with high energy efficiency. In this work, the performance of different kinds of preheaters for a castor oil biodiesel production are analyzed based on a second law analysis and an exergetic criteria. Analysis and design of heat exchangers requires to evaluate the entropy generation and/or exergy destruction as a consequence of the heat exchange and the pressure drop as a function of the design variables [23]. First proposal presented by West, in [12], is adapted to industrial conditions referred by Santana et.al [24] analyzing heat exchanger performance for castor oil biodiesel plant where it works as a preheater where castor oil requires heating with the aim of reduce viscosity and pump load. Several heat exchanger flow configurations have been evaluated in order to obtain the most appropriated one for the castor oil preheater.

2.2. Preheater performance and selection

Heat exchangers, one of the most common devices in industry, are used to move energy from one fluid to another [13]. Adequately use of a heat exchangers considers their design, thermal performance improvement, and volume – weight reduction [25]. In order to design and to check performance in heat exchangers, it can be used different approaches such as logarithmic mean temperature difference method ($LMTD$), heat exchanger effectiveness – number of transfer units method ($\varepsilon - NTU$), $\psi - P$ method and the $P_1 - P_2$ method. These methods are summarized in

(2-1). More details for each of them can be seen in [26]

$$\begin{pmatrix} heat \\ transfer \\ rate,\ q \end{pmatrix} = \begin{pmatrix} effectiveness \\ correction \\ factor \end{pmatrix} \times \begin{pmatrix} thermal \\ conductance \end{pmatrix} \times \begin{pmatrix} temperature \\ difference \end{pmatrix},$$

$$\begin{pmatrix} heat\ transfer \\ rate,\ q \end{pmatrix} = \begin{Bmatrix} \varepsilon C_{min} \triangle T_{max}\ in\ \varepsilon - NTU\ method \\ P_1 C_1 \triangle T_{max}\ in\ P - NTU\ method \\ FUA \triangle T_{lm}\ in\ LMTD\ method \\ \psi UA \triangle T_{max}\ in\ \psi - NTU\ method \end{Bmatrix}. \quad (2\text{-}1)$$

Each of these aforementioned methods require estimations of an effectiveness or a correlation factor as a function of design parameters. The expression factor is used to indicate a common first law of thermodynamics origin for both the effectiveness and correlation factor. Correction factor does not have the physical meaning that the effectiveness does. Each method involves a temperature difference, the maximum difference $\triangle T_{max}$ or the logarithmic-mean temperature difference $\triangle T_{lm}$.

2.2.1. $NTU - \varepsilon$ METHOD

The heat exchanger effectiveness – number of transfer units method ($NTU - \varepsilon$) is used to design heat exchangers as well as to check performance in operating installed devices. It is considered as a powerful method in heat exchangers operating under steady states conditions, using the effectiveness concept [27]. It assumes, hot fluid heat losses are gained by the coldest fluid, working with constant Prandtl and Reynolds numbers [27]. In $NTU - \varepsilon$ method, only inlet conditions need to be specified in order to estimate the outlet temperatures. It can be used in different kind of heat exchangers (i.e., parallel, counter, cross flows, shell-and-tube) [13].

Generally, the ($\varepsilon - NTU$) method is preferred to design heat exchangers where heat transfer rates have to be determined such as automotive, aircraft and air-conditioning applications. The LMTD method could be used for rating problems, however computations are tedious and it requires multiple iterations when outlet temperatures are unknown. Therefore, $\varepsilon - NTU$ offers a simplified

analysis and it can be easily used for thermodynamic modeling [13] which is this work purpose. Table **2-1** summarizes different effectiveness expression for heat exchangers here analyzed.

Table 2-1: Effectiveness expressions for some heat exchangers

Type of Heat Exchanger	$\varepsilon(\mathbf{NTU},\mathbf{R})$
Counterflow	$\varepsilon = \frac{1-\exp[-(1-R)NTU]}{1-R*\exp[-(1-R)NTU]}$
Parallel flow	$\varepsilon = \frac{1}{1+R}\{1-\exp[-(1+R)NTU]\}$
Crossflow, C_{min} mixed and C_{max} unmixed	$\varepsilon = 1-\exp\left[\frac{1-\exp(-R*NTU)}{R}\right]$
Crossflow, C_{max} mixed and C_{min} unmixed	$\varepsilon = \frac{1}{R}[1-\exp\{-R[1-\exp(-NTU)]\}]$
Crossflow, C_{max} and C_{min} mixed	$\varepsilon = \frac{1}{\frac{1}{1-\exp(-NTU)}+\frac{R}{1-\exp(-R*NTU)}-\frac{1}{NTU}}$
Crossflow, C_{max} and C_{min} unmixed	$\varepsilon = 1-\frac{\exp(-NTU)\int(1+R*NTU-\tau)\exp(-\tau)I_0\left(2\sqrt{\tau NTU}\right)d\tau}{R*NTU}$
1 to 2 shell-and-tube heat exchanger	$\varepsilon_{1-2} = \frac{1}{1+R+\left(1+R^2\right)^{1/2}\frac{1+\exp\left[-NTU\left(1-R^2\right)^2\right]}{1-\exp\left[-NTU\left(1-R^2\right)^2\right]}}$
n to 2n shell-and-tube heat exchanger	$\varepsilon_{n-2n} = \frac{\left(\frac{1-\varepsilon_{1-2}R}{1-\varepsilon_{1-2}}\right)^{Ntp}-1}{\left(\frac{1-\varepsilon_{1-2}R}{1-\varepsilon_{1-2}}\right)^{Ntp}-R}$
Inlets on opposite sides	$\varepsilon_{1-2} = \frac{1}{\frac{R+1}{2}-\sqrt{1+R^2}\left[\frac{1}{1-exp\left(NTU\sqrt{1+R^2}\right)}-\frac{1}{2}\right]}$
Parallel Serial Flow	$\varepsilon_{s\Leftrightarrow} = 1-\prod_{i=1}^{n}(1-\varepsilon_{s,i})$

2.2.2. MODELING CASTOR OIL THERMOPHYSICAL PROPERTIES

Castor oil is a fatty acid mixture which is principally conformed by ricinoleic acid. Table **2-2** shows the average composition of castor oil. Castor oil is a highly non-ideal fluid and its thermophysical properties are not well estimated yet, especially second derivative properties like heat capability, speed of sound, etc. Perdomo et. al. [19] have proposed a model based on a version of the statistical association fluid theory called $SAFT-\gamma$ [20], [21] to represent thermodynamical properties for fatty acids (FAs) and fatty acid alkyl esters (FAAEs). Same author model has shown to be versatile for different kinds of fatty acid alkyl ester mixtures and for any combination of them [28] due to its group contribution formulation. In this work, we have used this approach to model castor oil as a mixture of the fatty acids profile shown in table **2-1** extracted from [29].

How it was mentioned above, Castor oil is a mixture of H-FA (ricinoleic acid and dihydroxystearic acid) and commons FA (Linoleic, Oleic, Stearic, Palmitic, Eicosanoic and Linoleic acid).

Their molecular structures are very important in order to model them by $SAFT-\gamma$ approach [28].

Table 2-2: Castor oil composition [29]

Fatty acid	Composition (%)
Ricinoleic acid	90.2
Linoleic acid	4.4
Oleic acid	2.8
Stearic acid	0.9
Palmitic acid	0.7
Dihydroxystearic	0.5
Licosanoic acid	0.3
Linolenic acid	0.2

$SAFT-\gamma$ EoS is presented in term of four molecular contributions:

$$\frac{A}{NkT}=\frac{A^{IDEAL}}{NkT}+\frac{A^{MONO}}{NkT}+\frac{A^{CHAIN}}{NkT}+\frac{A^{ASSOC}}{NkT}, \tag{2-2}$$

where N is the number of chain molecules in the mixture, k is the Boltzmann constant and T is the temperature. Now, A^{IDEAL} is the ideal free energy, A^{MONO} is the residual free energy due to the monomer segments, A^{CHAIN} is the contribution due to the bonding of monomers required form a chain molecule and A^{ASSOC} describes the contribution to the free energy due to intermolecular association. The energy contributions per molecule are functions of the energies per segment and, as well as the total number of segments that comprise the respective i molecular specie in the system expressed by:

$$NS=\sum_{k=1}^{NG}\nu_{k,i}\nu_k^*\mathbf{s}_k, \tag{2-3}$$

Where s_k corresponds to the proportion of each spherical segment in group k that contributes to the overall properties of the molecule, and NG is the number of chemical groups present in molecule i. Hydroxilated fatty acids contain a type b site (partial positive charged hydrogen atom in the hydroxyl group), two type a in the hydroxyl group and, additionally, the same number and types of sites already considered in FAs. Notice that H-FA can associate either with other FAs or with itself. The Helmholtz free energy contribution due to association is given by [21]:

$$\frac{A^{ASSOC}}{NkT} = \sum_{i=1}^{NC} x_i \sum_{k=1}^{NG} \nu_{k,i} \sum_{a=1}^{NST_k} n_{ka} \left(\ln X_{ika} + \frac{1 - X_{ika}}{2} \right). \tag{2-4}$$

where n_{ka} is the number of associating type a sites in the group k, the first sum runs over species i, the second sum, over all group types NG, and the third sums over all sites types NST_k. The term X_{ika} is defined as the fraction of molecules i not bonded at a site of type a, which is located on a type k group. The fraction of molecules not bonded at a given site in a castor oil composed by a mixture of FAs and H-FAs is given by:

$$\begin{aligned} X_{i,aa,e} &= \left(1 + \sum_{j=1}^{N_{HFAMES}} \rho x_j \nu_{sa,j} n_{sa,H} X_{j,sa,H} \Delta_{i,j,aa,sa,eH} \right)^{-1}, \\ &\cdot \\ &\cdot \\ X_{i,sa,H} &= \left(1 + \sum_{j=1}^{NC} \left(\rho x_j \nu_{aa,j} n_{aa,H} X_{j,aa,H} \Delta_{i,j,sa,aa,eH} \right) + \left(\rho x_j \nu_{sa,j} n_{sa,e} X_{j,sa,e} \Delta_{i,j,sa,sa,eH} \right) \right)^{-1}. \end{aligned} \tag{2-5}$$

In Eq. (2-5), the subscripts *sa* and *aa* represents the $CHOH$ group for secondary alcohols (alkanols and enols) and the $COOH$ group for carboxylic acids respectively. $\Delta_{i,j,aa,sa,eH}$ and $\Delta_{i,j,sa,sa,eH}$ are quantities depending on the well depth of the square-well associative Hydrogen-bonding (HB) interaction, $\varepsilon^{HB}_{aa,sa,eH}$ and $\varepsilon^{HB}_{sa,sa,eH}$, as well as on the available volume between sites. For more detail to obtain Helmholtz free energy due to association, readers are referred to [19], [28]. In order to model castor oil by $SAFT-\gamma$ approach, the following set of parameters for each functional group are required: the hard sphere diameters for ester group σ_{aa} and secondary alcohol in H-FA σ_{sa}; the respective ranges and factor shapes λ_{aa}, s_{aa} and λ_{sa}, s_{aa}, the unlike parameter for cross energy $(\varepsilon_{aa,sa}/k)$. The aforementioned parameters values are given in Tables **2-3** and **2-4**.

Table 2-3: Individual group parameters for characteristic groups present in FA and H-FA for the $SAFT-\gamma$ EoS. The superscript (*) in the groups indicates that the values were taken from [19], otherwise from Ref. [21].

Group	v_k^*	s_k	$\sigma_{kk}\,(A^\circ)$	λ_{kk}	$\varepsilon_{kk}/_k\,(K)$	NST_k	$n_{k,e}$	$n_{k,H}$
$COOH$	3	0.644	2.806	1.538	269.285	2	2	1
$CHOH$	2^*	0.4953^*	2.9441^*	1.7240^*	297.2838^*	2	2	1
CH_3	1	0.6670	3.8100	1.4013	252.601	0	0	0
CH_2	1	0.3330	4.0270	1.6610	240.482	0	0	0
$CH=$	1	0.3700	3.5580	1.6970	315.343	0	0	0

Table 2-4: Cross group energy parameters $(\varepsilon_{kl}/_k)$ for the $SAFT-\gamma$ EoS for FAs groups. The superscript (*) indicates that the value of the interaction were taken from [19], (**) were obtained in this work, the others from Ref. [21].

Group	CH_3	CH_2	$CH=$	$COOH$	$CHOH$
CH_3	252.6010	261.5200	232.335	257.515	242.4059^*
CH_2	261.5200	240.4820	221.117	283497	265.3959^*
$CH=$	232.3350	221.1170	315.343	-	274.2938^*
$COOH$	257.515	283.497	-	269.285	301.255^{**}
$CHOH$	242.4059^*	265.3959^*	274.2938^*	301.255^{**}	297.2838^*

With respect to the unlike diameter and attractive ranges were fixed according to the combination rule given by:

$$\sigma_{kl} = \frac{(\sigma_{kk} + \sigma_{ll})}{2}, \tag{2-6a}$$

$$\lambda_{kl} = \frac{(\lambda_{kk}\sigma_{kk} + \lambda_{ll}\sigma_{ll})}{(\sigma_{kk} + \sigma_{ll})}. \tag{2-6b}$$

For a second law analysis, liquid density and isobaric heat capability are mainly required. Liquid density is obtained following the same procedure shown in Ref [19], and isobaric heat capability by the following set of thermodynamical relationships:

Table 2-5: Group contribution division in $SAFT-\gamma$ approach

	Fatty Acid							
Group	**Ricinoleic**	**Linoleic**	**Oleic**	**Stearic**	**Palmitic**	**Dihydroxystearic**	**Eicosanoic**	**Linolenic**
CH_3	1	1	1	1	1	1	1	1
CH_2	13	12	14	16	14	14	18	10
$CH=$	2	4	2	0	0	0	0	6
$CHOH$	1	0	0	0	0	2	0	0
$COOH$	1	1	1	1	1	1	1	1

$$\frac{C_v^r}{Nk} = -T^2\left(\frac{\partial^2 a^r}{\partial T^2}\right)_{V,N} - 2T\left(\frac{\partial a^r}{\partial T}\right)_{V,N}, \tag{2-7}$$

$$\left(\frac{\partial P}{\partial T}\right)_{T,N} = \left(\frac{P}{T}\right) - NkT\left(\frac{\partial^2 a^r}{\partial V \partial T}\right)_N, \tag{2-8}$$

$$\left(\frac{\partial P}{\partial V}\right)_{T,N} = -NkT\left(\frac{\partial^2 a^r}{\partial V^2}\right)_N, \tag{2-9}$$

$$C_v = C_V^{ideal} + C_V^r, \tag{2-10}$$

$$C_p = C_v - T\frac{\left(\frac{\partial P}{\partial T}\right)_V^2}{\left(\frac{\partial P}{\partial V}\right)_T}, \tag{2-11}$$

$$\beta_T^{-1} = \rho\left(\frac{\partial P}{\partial \rho}\right)_T. \tag{2-12}$$

$$\tag{2-13}$$

where C_v is the isochoric heat capability, C_p the isobaric heat capability which are required for first integral, and β_T is the isothermal compressibility coefficient required for the second integral of Eq (2-19). To apply $SAFT-\gamma$ approach to castor oil, molecules have to be divided into theirs constitutive small functional groups as it shown in Table **2-5**.

In order to estimate the pressure drop effects, dynamic viscosities and thermal conductivities are required for both fluids. All hot fluid properties (water in this case) are calculated from [30]. Castor oil viscosity is obtained as a function of temperature using a group contribution model based on empirical correlations proposed by Ceriani et.al. in [15], [16]. Castor oil thermal conductivity is calculated as a function of temperature using the experimental data of Ref [31]. It is worth mentioning that $SAFT-\gamma$ and the method presented by Ceriani, divide castor oil

molecules into different groups classifications.

2.2.3. THERMODYNAMICAL MODELING AND ANALYSIS FOR HEAT EXCHANGER SELECTION

Thermodynamic heat exchanger design enable us to identify the principal factors that affect effectiveness and to understand the thermodynamic efficiencies of heat exchangers. In this work, exergy and entropy are studied for different heat exchanger flow arrangements as criteria for evaluation/selection of a castor oil heat exchanger.

Entropy Generation

In heat exchanging processes, heat transfer and flow characteristics are determined by a phenomena called irreversibility. Shah, in [26], reduced heat transfer irreversibilities into five cases: a finite temperature difference, mixing of dissimilar fluids, fluid friction, phase change and flow throttling. For the heat exchangers here analyzed, irreversibilities due to finite temperature difference and fluid friction are taken into account for their major role. Different authors [26], [32]–[37] have shown expressions for maximun entropy generation (MEG) as a function of heat capability ratio, heat exchanger effectiveness (thus number of transfer unit and flow arrangement), as shown in Eq. 2-14. In this work, Eq. 2-14 only has two contributions; one due to the finite temperature differences and the other due to fluid friction that are described in Eqs. 2-15 and 2-16.

$$\frac{\dot{S}_{irr}}{C_{max}} = S^* = f\left(R, \varepsilon, \vartheta\right) = f\left(R, NTU, \vartheta, flow\,arrangement\right), \tag{2-14}$$

$$S^*_{FDT} = R\ln\left[1+\varepsilon\left(\vartheta^{-1}-1\right)\right] + \ln\left[1+\varepsilon R\left(\vartheta-1\right)\right]. \tag{2-15}$$

where ϑ is defined as the inlet temperature ratio ($\vartheta = {}^{T_{1,i}}/_{T_{2,i}}$). Fluid friction contribution has to be calculated for cold and hot fluids.

$$S^*_{FF} = \frac{\dot{m}\triangle P}{\rho C_{max} T_i} \cdot \frac{\ln\mid 1+\varepsilon\left(T_i^{-1}-1\right)\mid}{\varepsilon\left(T_i^{-1}-1\right)}. \tag{2-16}$$

Exergy Analysis

Exergy could be defined as a maximum useful work obtainable when the system interacts with its thermodynamic surroundings. For a material stream, exergy can be estimated as follows,

$$e = h - h_{\infty} - T_{\infty}\left(s - s_{\infty}\right). \tag{2-17}$$

For a fluid with mass rate, $\dot{m}$, the exergy variation from the heat exchanger inlet to outlet is given by:

$$\triangle E = \int_{inlet}^{outlet} \dot{m} C_P \left(1 - \frac{T_{\infty}}{T}\right) dT + \int_{inlet}^{outlet} \dot{m} \left[v - (T - T_{\infty}) \left(\frac{\partial v}{\partial T}\right)_P\right] dP \tag{2-18}$$

.

More detail about equation 2-18 derivation, see [23]. In order to introduce the exergy transfer effectiveness (ETE) which is defined as real exergy transfer and maximum exergy transfer in the heat exchanger ratio where maximum exergy occurs when cold fluid reaches hot fluid inlet temperature and there is no pressure drop. In this work, ETE is implemented for all heat exchangers shown in Table **2-1**, and integrated for the wide inlet to outlet conditions using Gaussian quadratures [38]. It is important to highlight that fluid thermophysical properties are evaluated for this wide range of conditions, and incompressible liquid approximation is not assumed to solve Eq. 2-19.

$$\varepsilon_e = \frac{\int_{inlet}^{outlet} \dot{m} C_P \left(1 - \frac{T_{\infty}}{T}\right) dT + \int_{inlet}^{outlet} \dot{m} \left[v - (T - T_{\infty}) \left(\frac{\partial v}{\partial T}\right)_P\right] dP}{\int_{Tci\,or\,Thi}^{Thi\,or\,Tci} \dot{m} C_P \left(1 - \frac{T_{\infty}}{T}\right) dT} \tag{2-19}$$

2.3. Operation conditions and calculation procedure

How it was mentioned, the inlet operation conditions are extracted from Ref [24], and listed in table **2-6**. All fluids thermodynamical properties are calculated at bulk temperature and the wall temperature is calculated as the mean of bulk temperatures of hot and cold fluids. ETE and MEG are calculated using the calculation scheme shown in Fig. **2-1**.

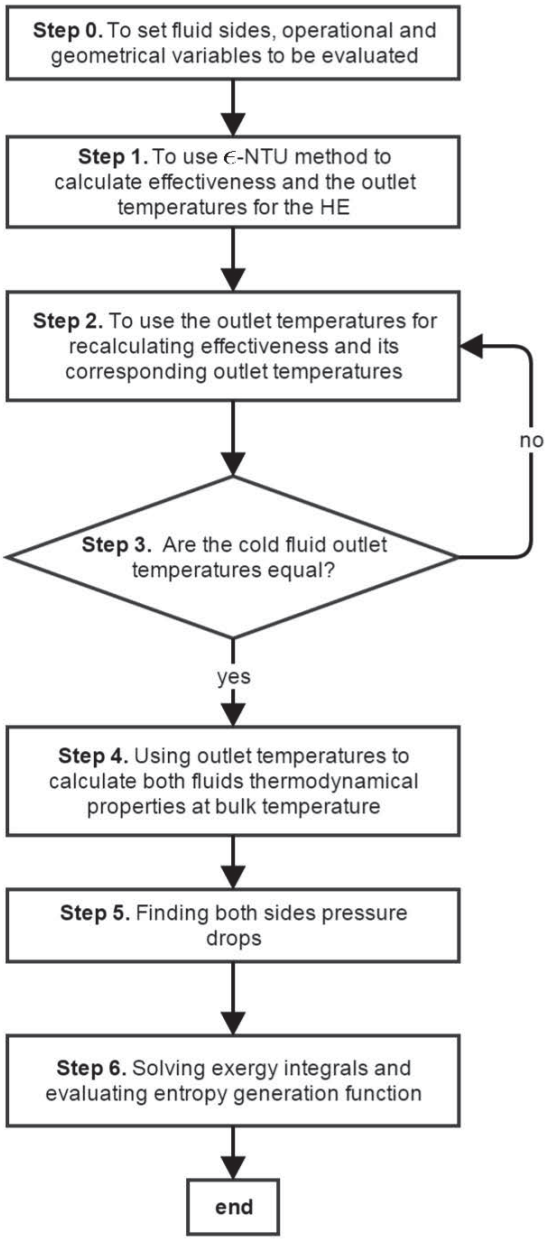

Figure 2-1: Scheme of calculation for ETE and EG.

Table 2-6: Inlet operation conditions Ref [24]

Condition	value	unit
Hot fluid mass flow rate	500	kg/s
Cold fluid mass flow rate	1000	kg/s
Hot fluid inlet temperature	90	^oC
Cold fluid inlet temperature	20	^oC
Hot fluid	Boiler Water	
Cold fluid	Castor oil	

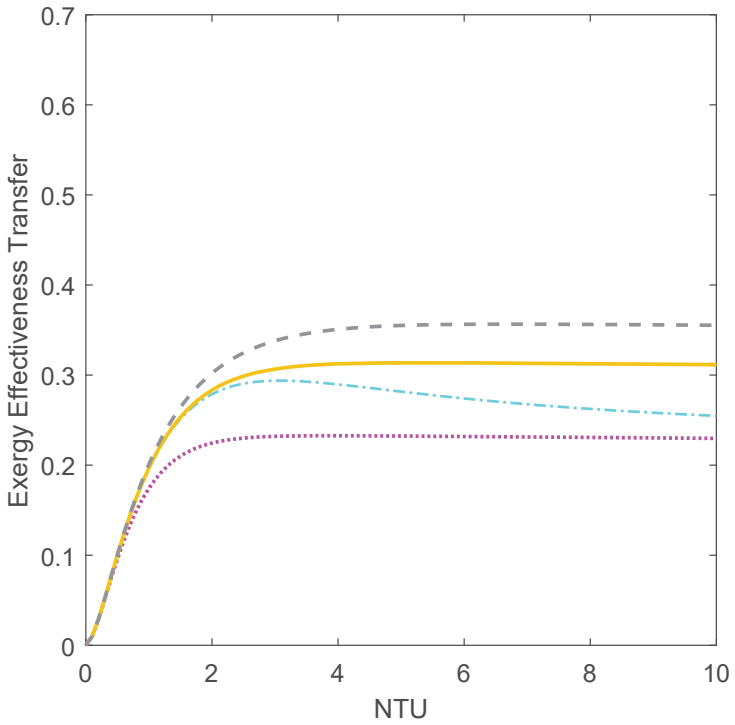

Figure 2-2: Cold fluid exergy transfer effectiveness vs NTU: (dotted line) Parallel flow, Crossflow (dash-dot line; both sides mixed), (solid line) Shell-&-tube 1 to 2 TEMA E, Crossflow (dashed line; Cmin unmixed and Cmax mixed).

Curves for cold fluid ETE as a function of NTU are shown in Figs. **2-2** and F**2-3** for different class of flow arrangement. Higher values for ETE are found for large NTU values due to the exit temperatures between cold and hot fluids are so close, but each flow arrangement has its maximun ETE. Counterflow and shell-&-tube show the higher ETE values than the other arraignments. Counterflow has the highest values of effectiveness, but it requires high values of NTU. By other hand, shell-&-tube reaches high ETE values for short NTU compared to counterflow arrangement. High NTU values are related with high heat transfer areas instead of high overall heat transfer coefficients, because real single phase heat exchanger overall heat transfer coefficients do not exceed 4500 W/m^2K [13].

Irreversibilities are an unfavorable effect over efficiency and thermal behavior of the heat exchanger. The EG curves ,Figs. **2-4** and **2-4**, show that entropy is highly generated for short NTU values due to a finite temperature difference and they have their maximum for a fixed value of NTU that depends on flow arrangement. From this maximum, EG decreases inasmuch temper-

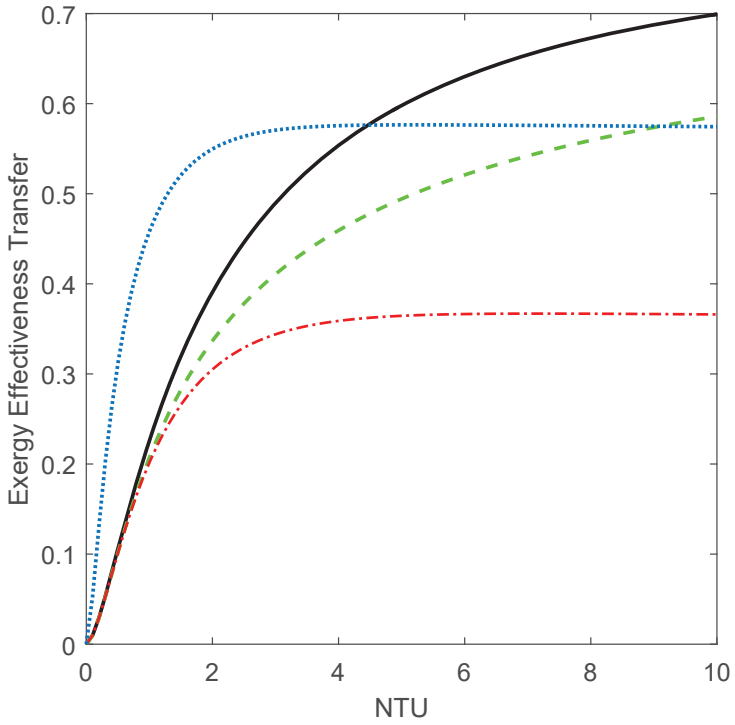

Figure 2-3: Cold fluid exergy transfer effectiveness vsNTU: (dotted line) Shell-&-tube 2 to 4 TEMA E, Crossflow (dash-dot line; Cmin mixed and Cmax unmixed), (solid line) Counterflow , Crossflow (dashed line; both sides unmixed).

ature difference between hot and cold fluids are closer each other. At this point, pressure drop starts to take an important role in entropy generation.

Counterflow arrangement shows the lowest values in term of EG for the different NTU values, but the Shell-&-tube configurations reach the lower values of EG for short NTU values. Feasible values of NTU cannot be short or high, so the better heat exchanger configuration is Shell-&-tube configuration. Useful work is notably affected by entropy generation because NTU values between 1.5 and 2.3 range the maximum values of ETE and the minimum values of EG. It is required to obtain more detailed calculations for Shell-&-tube heat exchangers in order to estimate better geometrical parameters and to determine their influence in ETE and EG. Detailed analysis requires calculations of ETE for both hot and cold fluids, and EG using rigourous design methods for Shell-&-tube heat exchangers.

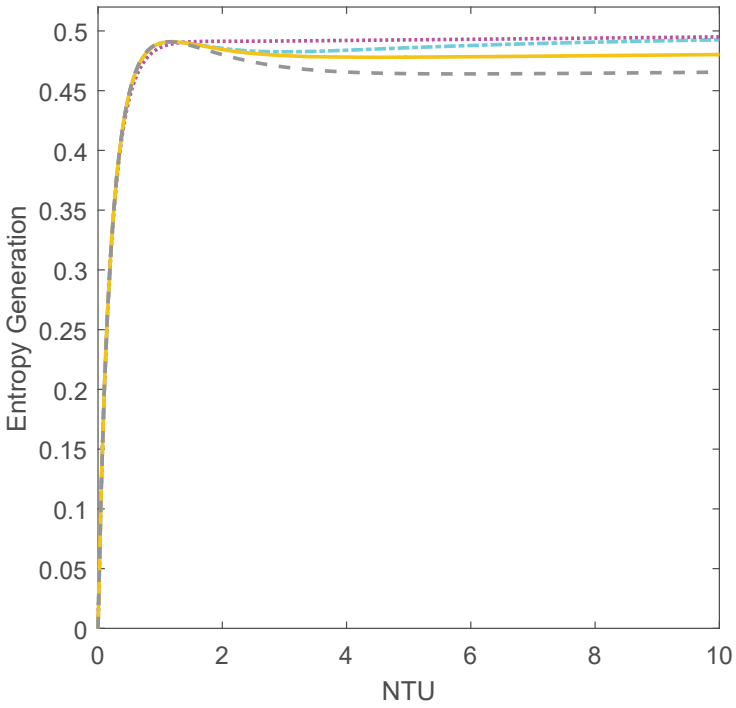

Figure 2-4: Cold fluid entropy generation vs NTU: (dotted line) Parallel flow, Crossflow (dash-dot line; both sides mixed), (solid line) Shell-&-tube 1 to 2 TEMA E, Crossflow (dashed line; Cmin unmixed and Cmax mixed).

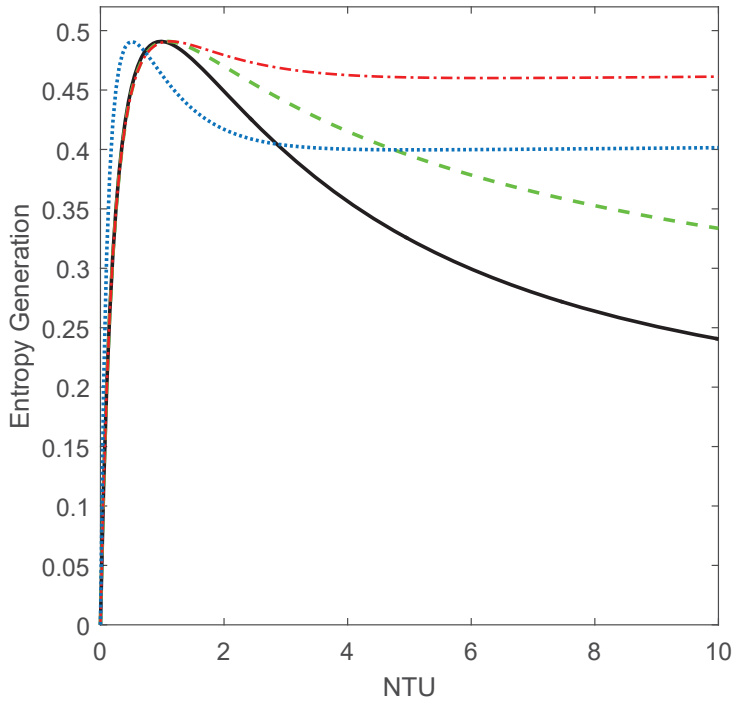

Figure 2-5: Cold fluid entropy generation vs NTU: (dotted line) Shell-&-tube 2 to 4 TEMA E, Crossflow (dash-dot line; Cmin mixed and Cmax unmixed), (solid line) Counterflow , Crossflow (dashed line; both sides unmixed).

2.3.1. SHELL-&-TUBE HEAT EXCHANGER THERMODYNAMICAL ANALYSIS

This kind of heat exchanger has a certain degree of complexity due to shell side flow. Many variables are involve from geometrical variables to hydrodynamic effects (flow leakage, bypass, etc). In this work, Bell-Delaware method (BDM) is used as a design method to consider all the aforementioned effects into shell side [39]. Calculations for exergy and entropy require accurate pressure drop estimations for both tube and shell sides for a real thermal analysis predictions [26].

Tube side pressure drop and heat transfer coefficient

Castor oil is chosen as the tube side fluid because of its high value for viscosity. Tube side pressure drop effect can be divide into different contribution as Eq. (2-20) shows. Pressure drop calculations, used in this work, contain all contributions shown in (2-20). Entrance and exit pressure lost coefficients for a multiple circular tube core are obtained, extracting data from [40] and generating an empirical equation as a function of σ (ratio of core minimum free flow area to frontal area) and *Re* number.

$$\frac{\triangle p}{p_i} = \frac{\dot{m}^2}{2g_c\rho_i p_i A^2}\left[\underbrace{1-\sigma^2+k_c}_{entrance\,effect} + \underbrace{2\left(\frac{\rho_i}{\rho_o}-1\right)}_{momentun\,effect} + \underbrace{f\frac{L}{r_h}\rho_i\left(\frac{1}{\rho}\right)_m}_{core\,friction} - \underbrace{\left(1-\sigma^2-k_e\right)\frac{\rho_i}{\rho_o}}_{exit\,effect}\right]. \quad (2\text{-}20)$$

Heat transfer coefficient are obtained using empirical correlations extracted from Ref [13], as follow

$$Nu_t = \begin{cases} 0.027Re_t^{4/5}Pr_t^{1/3}\phi_t^{0.14}, & Re_t > 10000 \\ 1.86(Re_tPr_t./(L/d_i))^{1/3}\phi_t^{0.14} & Re_t \leq 10000. \end{cases} \quad (2\text{-}21)$$

Shell side pressure drop and heat transfer coefficient

In the Bell-Delaware method, the shell heat transfer coefficient is calculated using Eq. 2-22. It depends on a different set of *J* values that are related with fluid movement thought the shell.

$$h_{shell} = h_{id} J_c J_l J_b J_s J_r. \tag{2-22}$$

The Shell side pressure drop is affected by leakage and bypass effects. Three terms are considered in the BD method for pressure drop calculations related with baffle, window and inlet-outlet shell parts [13].

$$\Delta P_{shell} = \left[(N_b - 1) \Delta P_{bid} \zeta_b + N_b \Delta P_{wid} \right] \zeta_l + 2 \Delta P_{bid} \left(1 + \frac{N_{rcw}}{N_{rcc}} \right) \zeta_b \zeta_s. \tag{2-23}$$

Tube and shell sides velocities where fixed as 3.1 and 2.1 respectively. These values are assumed in the range of 3 to 8 ft/s for tube side and 2 to 5 ft/s for shell side, in order to equilibrate high fouling rates at low velocities and erosion at high velocities [26]. Different set of shell-&-tube geometrical parameter are studied in this work in order to chose a good enough configuration that simultaneously reaches high values of ETE and low values for EG. The different set of configurations are listed in Table **2-7**. Each configuration has its own ETE and EG behavior as a function of NTU. ETE and EG scheme of calculation for a Shell-&-tube heat exchanger is shown in Fig (**2-6**).ETE calculations for each configuration are shown in Fig (**2-7**) which contains ETE for hot fluid (**2-7**,a) and (**2-7**,b) for cold fluid.

All curves reach a maximum value of ETE for a fixed value of NTU; at this point pressure drop starts to play the principal roll in ETE due to high areas despite outlet temperatures are close to inlet temperatures (Tho close to Tci), fluid friction is very high and exergy transfer is so inefficient. Higher value of ETE is reached by configuration 1 which uses the low value of tube diameter, and higher tube passes. It is important to highlight that recommended values for tube pitch, and baffle cut in literature [13], [26] are chosen in configuration 1 and then there is an thermal design explanation of this empirical criteria values in term of exergy. By other side, worst configuration (in term of ETE) is number 3 that has the lowest value of tube passes. Results shows that tube passes increases ETE values.

In addition to ETE, EG calculations show that entropy has a local maximum for low values of NTU how was discussed in section 2.3. Pressure drop start to increase EG until a local minima is

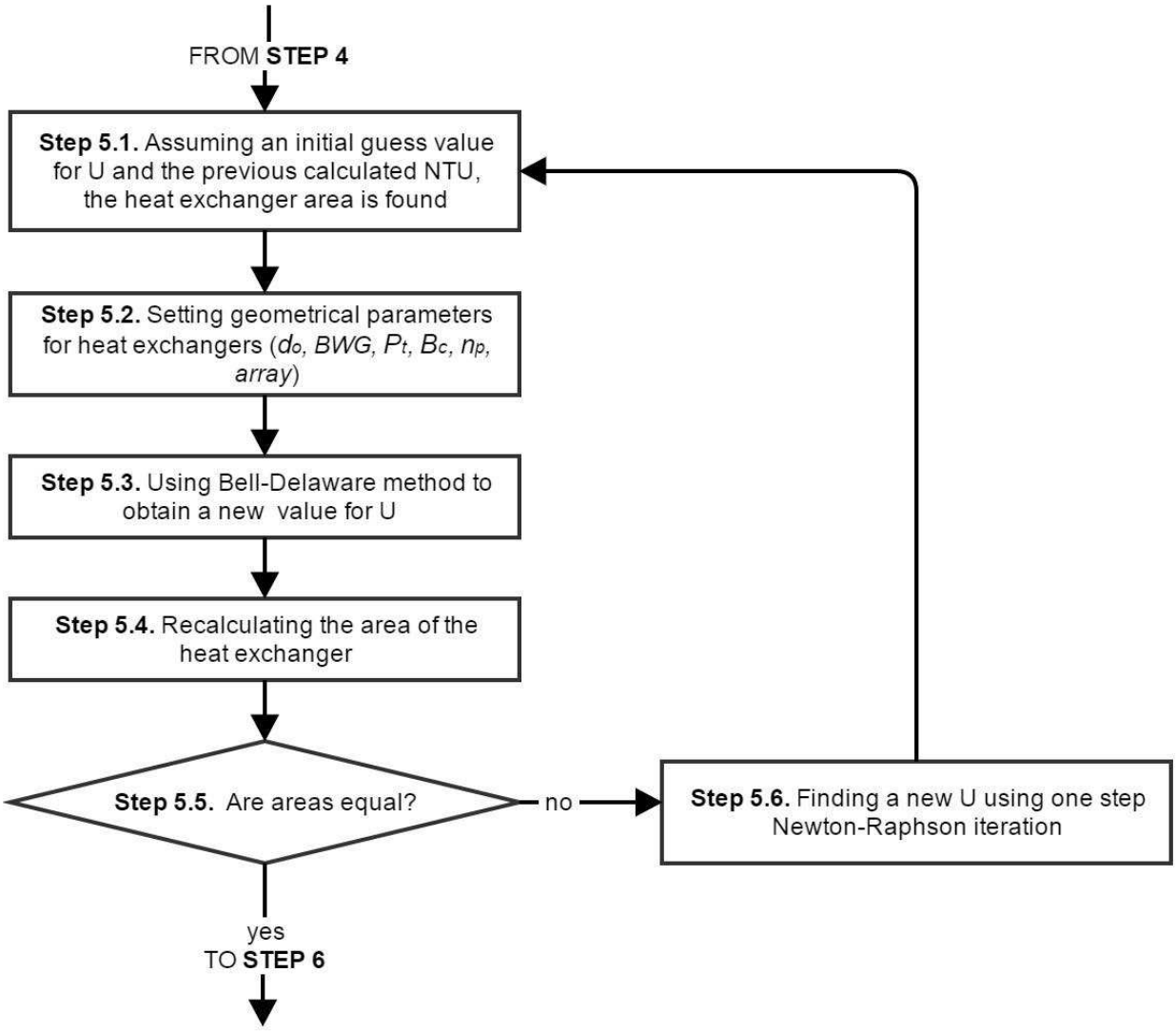

Figure 2-6: Scheme of calculation for ETE and EG in Shell-&-tube heat exchangers.

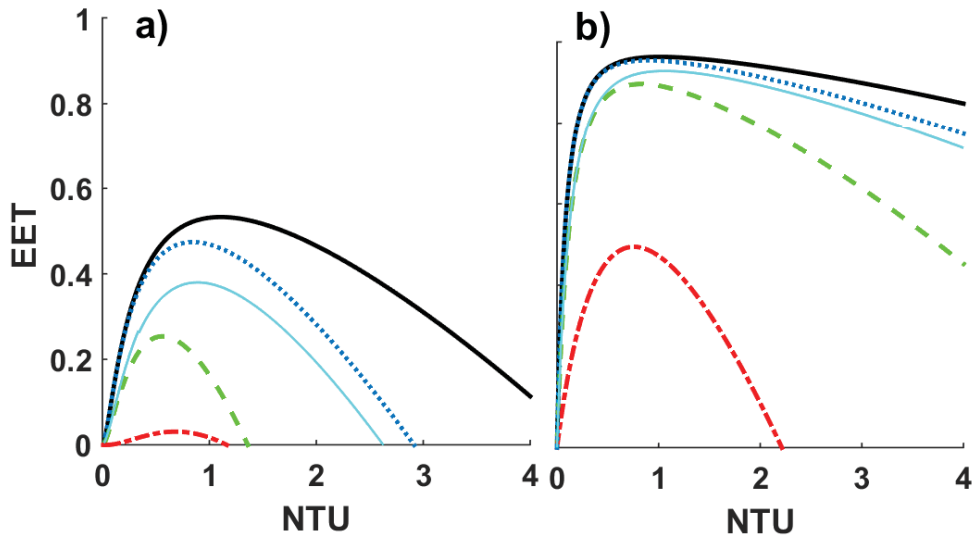

Figure 2-7: Effectiveness Transfer Exergy vs NTU for Shell-&-tube heat exchangers: a) Cold fluid b) Hot fluid. (solid line) Configuration 1, (dashed line) Configuration 2, (dash-dot line) Configuration 3, (dotted line) Configuration 4, (tight solid line) Configuration 5

Table 2-7: Shell-&-Tube HE configurations

CONFIGURATION	**PARAMETERS**					
	Arrangement	$\mathbf{P_t}$	**Baffle cut**	$\mathbf{d \times 10^{-3}}[m]$	**Wall thicknes** $\times \mathbf{10^{-3}}[m]$	$\mathbf{n_p}$
1	90^o	1.25	25%	6.35	0.406	6
2	45^o	1.4	15%	9.53	1.245	4
3	30^o	1.5	20%	9.53	0.559	2
4	45^o	1.3	30%	12.7	0.711	6
5	30^o	1.2	40%	9.53	0.559	4

found. Minimum values for each configuration are shown in Fig (**2-8**) where dimensionless EG is plotted as a function of NTU. Lower values of EG are preferred in order to obtain the less possible rate of irreversibility production. Configurations 2 and 5 have the same number of tube passes but pretty different values for pitch, so it can see the differences in EG behaviour. Configuration 3 presents a discontinuity close to NTU = 2.1 due to heat transfer coefficients and pressure drop empirical correlations are fractionated functions of Reynolds number and in this zone there is a flow regimen change. Figures (**2-7**) and (**2-8**) coincide in optimal regions of NTU; lower values of EG and higher values of ETE. In both cases, configuration 1 has obtained the optimal values than the others.

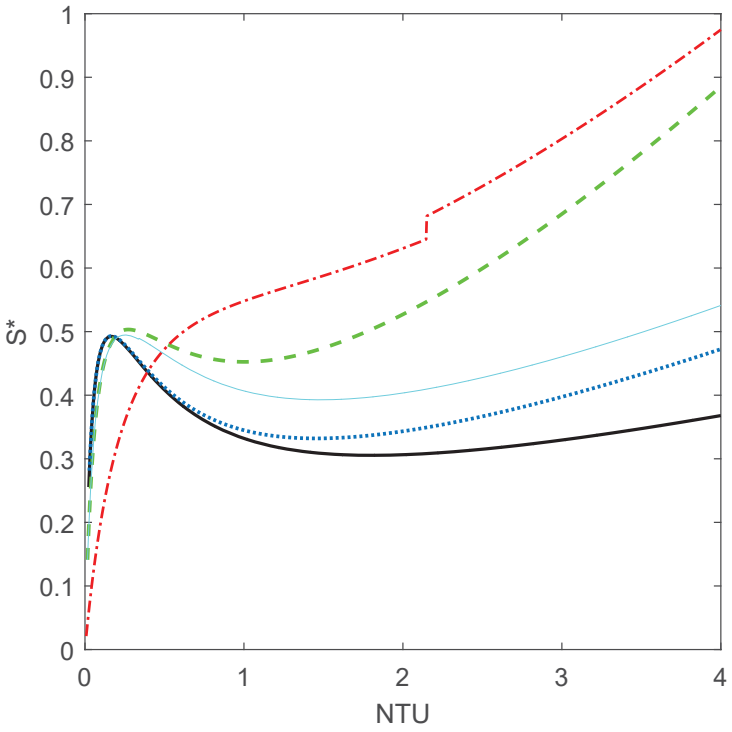

Figure 2-8: Dimensionless Entropy Generation vs NTU for Shell-&-tube heat exchangers: a) Cold fluid b) Hot fluid. (solid line) Configuration 1, (dashed line) Configuration 2, (dash-dot line) Configuration 3, (dotted line) Configuration 4, (tight solid line) Configuration 5

2.4. Conclusions

This study was done in order to develop a thermal analysis based on exergy efficiency and entropy generation in a heat exchanger used for preheat a castor oil feed stock before to get int a reactor. Required castor oil thermophysical properties have been obtained using a molecular model based on $SAFT-\gamma$ approach. Exergy transfer effectiveness (ETE) and Entropy generation (EG) as a function of NTU have been obtained for different heat exchanger flow arrangements where counter flow and Shell-&-tube flow reached the optimal value in terms of ETE and EG. For intermediate values of NTU, Shell-&-tube flow shows most feasible values of ETE and EG.

The Bell-Delaware method has been used as rigorous heat exchanger design method in order to obtain pressure drops and global heat transfer coefficient in Shell-&-tube heat exchangers. Five different geometrical configurations have been studied in order to determine the better option in terms of ETE and EG; configuration 1 has the higher ETE and the lower EG values for a feasible NTU. Configuration 1 has the recommended pitch ratio 1.25 and 25% Baffle cutoff in term of

fluid flow and mechanical aspects which are in very good agreement with exergy and second law analysis.

It is known that multiple tube passes increases the heat exchanger capital cost, so optimum value of thermodynamic behavior could not match with cost optimum. There is necessary an thermo-economical optimization to implement this approach to real life design problems. It is necessary to obtain an optimization function for the dual problem (maximun EET - minimum EG) as a function of the different set of geometrical parameters.

2.5. Nomenclature

P	, Pressure	$[Pa]$
q	, Heat Transfer Rate	$[W]$
C	, Specific Heat	$[J/kgK]$
T	, Temperature	$[K]$
F	, Logarithmic Mean Temperature Difference correction factor	dimensionless
U	, Overall heat transfer coefficient	$[W/m^2K]$
Ao	, Heat transfer area	$[m^2]$
R	, C_{min}/C_{max}	dimensionless
$\dot{m}$	, Mass flow rate	$[kg/s]$
g_c	, Dimensional constant	$[kgm/Ns^2]$
k	, Loss coefficient for flow at heat exchanger entrance	dimensionless
f	, Fanning friction factor	dimensionless
L	, Length	$[m]$
r	, Radius	$[m]$
N	, Number, molecular number	dimensionless
n	, Number	dimensionless
S	, Entropy	$[J/K]$
h	, Specific enthalpy	$[J/kg]$
s	, Specific entropy	$[J/kgK]$
s_k	, Shape factor of k group	dimensionless
E	, Exergy	$[J]$
v	, Specific volume	$[m^3/kg]$
A	, Helmholtz energy	$[J]$
A^{IDEAL}	, Ideal energy of a chain molecules mixture	dimensionless
A^{MONO}	, Monomer energy of a chain molecules mixture	dimensionless
A^{CHAIN}	, Chain energy of a chain molecules mixture	dimensionless
A^{ASSOC}	, Association energy of a chain molecules mixture	dimensionless
A^{BOND}	, Bond information energy of a chain molecules mixture	dimensionless

N	, Molecular numbers	dimensionless
k	, Boltzmann constant	$[m^2kg/s^2/K^1]$
s	, Spherical segment	dimensionless
X_{ika}	, Molecular fraction of species i not bonded at a site of type a which is located on a type k group	dimensionless
x_i	, Molar fraction of i component	dimensionless
exp	, Euler function	dimensionless

2.5.1. SYMBOLS

ε	, Effectiveness	dimensionless
Δ	, Change	
$\Delta_{ij,kl,ab}$	, Function of association strength between sites a and b located on groups k and l of components i and j	
ψ	, $\Delta T_m/(T_{h,i}-T_{c,i})$	dimensionless
ρ	, Density	$[kg/m^3]$
σ	, Ratio of free flow area to frontal area	dimensionless
τ	, Dummy variable itegrated from 0 to $NTU \times R$	
ϑ	, Inlet temperature ratio	dimensionless
$\nu_{k,i}$	, Number of groups of type k in the molecule i	dimensionless
ν_k^*	, Number of segments that comprises ten k group	dimensionless
μ_{ka}	, Number of associationg type a sites in the group k	dimensionless
λ_{kl}	, Range of segment - segment SW interaction	dimensionless
σ_{kl}	, Contact diameter between k and l segments	dimensionless
β	, Compressibility coefficient	$[1/K]$
ϕ	, μ_w/μ_s	dimensionless
ε_{kl}	, Energy depth of the segment - segment interaction.	$[J]$

2.5.2. SUPERSCRIPTS

$*$ Normalized, dimensionless

2.5.3. SUBSCRIPTS

min	Minimum
max	Maximum
lm	Logarithmic mean
$1, i$	Inlet
$2, o$	Outlet
c	Contraction
e	Expansion
h	Hydraulic
m	Mean
t	Tube
s	Shell
p	Passes
irr	Irreversibilities
∞	Surroundings
sa	CHOH group for secondary alcohols
aa	COOH group for carboxylic acids
T	Isothermal
s	Serial
V	Isochoric
id	Ideal
b	Baffle
w	Window
l	Leak
i, j	Component
H	Proton-donor type association site
e	Proton-accepting type association site

2.5.4. ABBREVIATIONS

$TEMA$	Tubular Exchanger Manufacturers Association
$SAFT$	Statistical Associating Fluid Theory
$FAAE$	Fatty Acid Alkyl Esters
ETE	Exergy Transfer Effectiveness
MEG	Maximum Entropy Generation
EG	Entropy Generation
$H-FA$	Hydroxyl Fatty Acid
FA	Fatty Acid
$LMTD$	Logarithmic Mean Temperature Difference
NTU	Number of Transfer Units
FDT	Finite Temperature Difference
FF	Fluid Flow
NG	Number of Chemical Groups Present in Molecule
NC	Number of Chemical Compunds
NS	Number of Segments
NST_k	Number of Sites of k Type in Molecule
EoS	Equation of State
HB	Hydrogen-Bonding
SW	Square Well Potential
$H-FAME$	Fatty Acid Methyl Esters With Hydroxy Group
$ASTM$	American Society for Testing And Materials

Bibliography

[1] K. Ramezani, S. Rowshanzamir, and M. H. Eikani, "Castor oil transesterification reaction: A kinetic study and optimization of parameters", *Energy*, vol. 35, no. 10, pp. 4142–4148, 2010, ISSN: 0360-5442. DOI: http://dx.doi.org/10.1016/j.energy.2010.06.034. [Online]. Available: http://www.sciencedirect.com/science/article/pii/S0360544210003579.

[2] G. Knothe, "Biodiesel and renewable diesel: A comparison", *Progress in Energy and Combustion Science*, vol. 36, no. 3, pp. 364–373, 2010, ISSN: 0360-1285. DOI: http://dx.doi.org/10.1016/j.pecs.2009.11.004. [Online]. Available: http://www.sciencedirect.com/science/article/pii/S0360128509000677.

[3] L. S. Severino, D. L. Auld, M. Baldanzi, M. J. D. Cândido, G. Chen, W. Crosby, D. Tan, X. He, P. Lakshmamma, C. Lavanya, O. L. T. Machado, T. Mielke, M. Milani, T. D. Miller, J. B. Morris, S. A. Morse, A. A. Navas, D. J. Soares, V. Sofiatti, M. L. Wang, M. D. Zanotto, and H. Zieler, *A Review on the Challenges for Increased Production of Castor*, Jul. 2012. [Online]. Available: https://dl.sciencesocieties.org/publications/aj/abstracts/104/4/853.

[4] D. S. Ogunniyi, "Castor oil: A vital industrial raw material", *Bioresource Technology*, vol. 97, no. 9, pp. 1086–1091, 2006, ISSN: 0960-8524. DOI: http://dx.doi.org/10.1016/j.biortech.2005.03.028. [Online]. Available: http://www.sciencedirect.com/science/article/pii/S0960852405002026.

[5] A. K. Agarwal, "Biofuels (alcohols and biodiesel) applications as fuels for internal combustion engines", *Progress in Energy and Combustion Science*, vol. 33, no. 3, pp. 233–271, 2007, ISSN: 0360-1285. DOI: http://dx.doi.org/10.1016/j.pecs.2006.08.003.

[Online]. Available: http://www.sciencedirect.com/science/article/pii/S0360128506000384.

[6] S. M. P. Meneghetti, M. R. Meneghetti, C. R. Wolf, E. C. Silva, G. E. S. Lima, L. de Lira Silva, T. M. Serra, F. Cauduro, and L. G. de Oliveira, "Biodiesel from Castor Oil: A Comparison of Ethanolysis versus Methanolysis", *Energy & Fuels*, vol. 20, no. 5, pp. 2262–2265, 2006. DOI: 10.1021/ef060118m. [Online]. Available: http://dx.doi.org/10.1021/ef060118m.

[7] G. Knothe, ""DESIGNER" BIODIESEL: OPTIMIZING FATTY ESTER COMPOSITION TO IMPROVE FUEL PROPERTIES†", *Energy & Fuels*, vol. 22, no. 2, pp. 1358–1364, 2008. DOI: 10.1021/ef700639e. [Online]. Available: http://dx.doi.org/10.1021/ef700639e.

[8] M. J. Haas, A. J. McAloon, W. C. Yee, and T. A. Foglia, "A process model to estimate biodiesel production costs", *Bioresource Technology*, vol. 97, no. 4, pp. 671–678, 2006, ISSN: 0960-8524. DOI: http://dx.doi.org/10.1016/j.biortech.2005.03.039. [Online]. Available: http://www.sciencedirect.com/science/article/pii/S0960852405001938.

[9] W. D. Y.M. Sani and a.R. Abdul Aziz, "Biodiesel Feedstock and Production Technologies : Successes , Challenges and Prospects", in *Biodiesel - Feedstocks, Production and Applications*, 2012, pp. 77–101, ISBN: 978-953-51-0910-5. DOI: 10.5772/52790. [Online]. Available: http://www.intechopen.com/books/authors/biodiesel-feedstocks-production-and-applications/biodiesel-feedstock-and-production-technologies-successes-challenges-and-prospects-.

[10] M. Canakci and J. V. Gerpen, "Biodiesel Production Via Acid Catalysis", *Transactions of the ASAE (American Society of Agricultural Engineers)*, vol. 42, no. 1984, pp. 1203–1210, 1999.

[11] T. M. Y. Khan, A. E. Atabani, I. A. Badruddin, A. Badarudin, M. S. Khayoon, and S. Triwahyono, "Recent scenario and technologies to utilize non-edible oils for biodiesel production", *Renewable and Sustainable Energy Reviews*, vol. 37, no. 0, pp. 840–851, 2014, ISSN: 1364-0321. DOI: http://dx.doi.org/10.1016/j.rser.2014.05.064.

[Online]. Available: http://www.sciencedirect.com/science/article/pii/S136403211400389X.

[12] A. H. West, D. Posarac, and N. Ellis, "Assessment of four biodiesel production processes using HYSYS.Plant", *Bioresource Technology*, vol. 99, no. 14, pp. 6587–6601, 2008, ISSN: 0960-8524. DOI: http://dx.doi.org/10.1016/j.biortech.2007.11.046. [Online]. Available: http://www.sciencedirect.com/science/article/pii/S0960852407009686.

[13] S. Kakac, H. Liu, and A. Pramuanjaroenkij, *Heat exchangers: selection, rating, and thermal design*. CRC press, 2012.

[14] W. Yuan, A. Hansen, and Q. Zhang, "Predicting the physical properties of biodiesel for combustion modeling", *Transactions of the American Society of Agricultural Engineers*, vol. 46, no. 6, pp. 1487–1493, 2003, cited By 92. [Online]. Available: https://www.scopus.com/inward/record.uri?eid=2-s2.0-1542754617&partnerID=40&md5=69586992873874ae58026a4d8e8f09b7.

[15] R. Ceriani, C. B. Gonçalves, J. Rabelo, M. Caruso, A. C. C. Cunha, F. W. Cavaleri, E. A. C. Batista, and A. J. A. Meirelles, "Group contribution model for predicting viscosity of fatty compounds", *Journal of Chemical & Engineering Data*, vol. 52, no. 3, pp. 965–972, 2007. DOI: 10.1021/je600552b. eprint: http://dx.doi.org/10.1021/je600552b. [Online]. Available: http://dx.doi.org/10.1021/je600552b.

[16] R. Ceriani, C. B. Gonçalves, and J. A. P. Coutinho, "Prediction of viscosities of fatty compounds and biodiesel by group contribution", *Energy & Fuels*, vol. 25, no. 8, pp. 3712–3717, 2011. DOI: 10.1021/ef200669k. eprint: http://dx.doi.org/10.1021/ef200669k. [Online]. Available: http://dx.doi.org/10.1021/ef200669k.

[17] M. L. Huber, E. W. Lemmon, A. Kazakov, L. S. Ott, and T. J. Bruno, "Model for the thermodynamic properties of a biodiesel fuel", *Energy & Fuels*, vol. 23, no. 7, pp. 3790–3797, 2009. DOI: 10.1021/ef900159g. eprint: http://dx.doi.org/10.1021/ef900159g. [Online]. Available: http://dx.doi.org/10.1021/ef900159g.

[18] M. B. Oliveira, V. Ribeiro, A. J. Queimada, and J. A. P. Coutinho, "Modeling phase equilibria relevant to biodiesel production: A comparison of gE models, cubic EoS, EoS gE and association EoS", *Industrial & Engineering Chemistry Research*, vol. 50, no. 4, pp. 2348–2358, 2011. DOI: 10.1021/ie1013585. [Online]. Available: https://doi.org/10.1021/ie1013585.

[19] F. A. Perdomo, B. M. Millán, and J. L. Aragón, "Predicting the physical–chemical properties of biodiesel fuels assessing the molecular structure with the SAFT γ group contribution approach", *Energy*, vol. 72, no. 0, pp. 274–290, 2014, ISSN: 0360-5442. DOI: http://dx.doi.org/10.1016/j.energy.2014.05.035. [Online]. Available: http://www.sciencedirect.com/science/article/pii/S036054421400601X.

[20] A. Lymperiadis, C. S. Adjiman, A. Galindo, and G. Jackson, "A group contribution method for associating chain molecules based on the statistical associating fluid theory (SAFT-γ)", *The Journal of Chemical Physics*, vol. 127, no. 23, pp. –, 2007. DOI: http://dx.doi.org/10.1063/1.2813894. [Online]. Available: http://scitation.aip.org/content/aip/journal/jcp/127/23/10.1063/1.2813894.

[21] A. Lymperiadis, C. S. Adjiman, G. Jackson, and A. Galindo, "A generalisation of the SAFT- group contribution method for groups comprising multiple spherical segments", *Fluid Phase Equilibria*, vol. 274, no. 1–2, pp. 85–104, 2008, ISSN: 0378-3812. DOI: http://dx.doi.org/10.1016/j.fluid.2008.08.005. [Online]. Available: http://www.sciencedirect.com/science/article/pii/S0378381208002458.

[22] A. Bejan, G. Tsatsaronis, and M. Moran, *Thermal Design and Optimization*, ser. Wiley-Interscience publication. Wiley, 1996, ISBN: 9780471584674. [Online]. Available: https://books.google.com.co/books?id=sTi2crXeZYgC.

[23] S.-Y. Wu, X.-F. Yuan, Y.-R. Li, and L. Xiao, "Exergy transfer effectiveness on heat exchanger for finite pressure drop", *Energy*, vol. 32, no. 11, pp. 2110–2120, 2007, ISSN: 0360-5442. DOI: http://dx.doi.org/10.1016/j.energy.2007.04.010. [Online]. Available: http://www.sciencedirect.com/science/article/pii/S036054420700076X.

[24] G. C. S. Santana, P. F. Martins, N. de Lima da Silva, C. B. Batistella, R. M. Filho, and M. R. W. Maciel, "Simulation and cost estimate for biodiesel production using castor

oil", *Chemical Engineering Research and Design*, vol. 88, no. 5–6, pp. 626–632, 2010, ISSN: 0263-8762. DOI: http://dx.doi.org/10.1016/j.cherd.2009.09.015. [Online]. Available: http://www.sciencedirect.com/science/article/pii/S0263876209002536.

[25] Q. Chen, "Entransy dissipation-based thermal resistance method for heat exchanger performance design and optimization", *International Journal of Heat and Mass Transfer*, vol. 60, no. 0, pp. 156–162, 2013, ISSN: 0017-9310. DOI: http://dx.doi.org/10.1016/j.ijheatmasstransfer.2012.12.062. [Online]. Available: http://www.sciencedirect.com/science/article/pii/S0017931013000173.

[26] R. K. Shah and D. P. Sekulic, *Fundamentals of heat exchanger design*. John Wiley & Sons, 2003.

[27] S. Lalot, "Heat Exchangers: Types, Design, and Applications", in *Heat Exchangers: Types, Design, and Applications*, S. T. Branson, Ed., New York: Nova Science Publishers, Inc, 2011, ch. Chapter 2, pp. 43–113, ISBN: 978-1-61761-308-1.

[28] L. Perdomo, F. A. Perdomo, B. M. Millán, and J. L. Aragón, "Design and improvement of biodiesel fuels blends by optimization of their molecular structures and compositions", *Chemical Engineering Research and Design*, vol. 92, no. 8, pp. 1482–1494, 2014, ISSN: 0263-8762. DOI: http://dx.doi.org/10.1016/j.cherd.2014.02.011. [Online]. Available: http://www.sciencedirect.com/science/article/pii/S0263876214000914.

[29] M. M. Conceição, R. A. Candeia, F. C. Silva, A. F. Bezerra, V. J. F. Jr., and A. G. Souza, "Thermoanalytical characterization of castor oil biodiesel", *Renewable and Sustainable Energy Reviews*, vol. 11, no. 5, pp. 964–975, 2007, ISSN: 1364-0321. DOI: http://dx.doi.org/10.1016/j.rser.2005.10.001. [Online]. Available: http://www.sciencedirect.com/science/article/pii/S1364032105000961.

[30] C. Yaws, *Chemical Properties Handbook: Physical, Thermodynamics, Environmental Transport, Safety & Health Related Properties for Organic &*. McGraw-Hill Professional, 1999.

[31] G. W. C. Kaye and W. F. Higgins, "The thermal conductivities of certain liquids", *Proceedings of the Royal Society of London A: Mathematical, Physical and Engineering Sciences*, vol. 117, no. 777, pp. 459–470, 1928, ISSN: 0950-1207. DOI: 10.1098/rspa.1928.0010.

eprint: http://rspa.royalsocietypublishing.org/content/117/777/459.full.pdf. [Online]. Available: http://rspa.royalsocietypublishing.org/content/117/777/459.

[32] R. L. Cornelissen and G. G. Hirs, "Exergetic optimisation of a heat exchanger", *Energy Conversion and Management*, vol. 38, no. 15–17, pp. 1567–1576, 1997, ISSN: 0196-8904. DOI: http://dx.doi.org/10.1016/S0196-8904(96)00218-X. [Online]. Available: http://www.sciencedirect.com/science/article/pii/S019689049600218X.

[33] J. E. Hesselgreaves, "Rationalisation of second law analysis of heat exchangers", *International Journal of Heat and Mass Transfer*, vol. 43, no. 22, pp. 4189–4204, 2000, ISSN: 0017-9310. DOI: http://dx.doi.org/10.1016/S0017-9310(99)00364-6. [Online]. Available: http://www.sciencedirect.com/science/article/pii/S0017931099003646.

[34] R. Oğulata, F. Doba, and T. Yilmaz, "Irreversibility analysis of cross flow heat exchangers", *Energy Conversion and Management*, vol. 41, no. 15, pp. 1585–1599, 2000, ISSN: 0196-8904. DOI: http://dx.doi.org/10.1016/S0196-8904(00)00020-0. [Online]. Available: http://www.sciencedirect.com/science/article/pii/S0196890400000200.

[35] R. K. Shah and T. Skiepko, "Entropy Generation Extrema and Their Relationship With Heat Exchanger Effectiveness—Number of Transfer Unit Behavior for Complex Flow Arrangements", *Journal of Heat Transfer*, vol. 126, no. 6, pp. 994–1002, Jan. 2005, ISSN: 0022-1481. [Online]. Available: http://dx.doi.org/10.1115/1.1846694.

[36] J. Guo, L. Cheng, and M. Xu, "Optimization design of shell-and-tube heat exchanger by entropy generation minimization and genetic algorithm", *Applied Thermal Engineering*, vol. 29, no. 14–15, pp. 2954–2960, 2009, ISSN: 1359-4311. DOI: http://dx.doi.org/10.1016/j.applthermaleng.2009.03.011. [Online]. Available: http://www.sciencedirect.com/science/article/pii/S1359431109000921.

[37] M. Mishra, P. K. Das, and S. Sarangi, "Second law based optimisation of crossflow plate-fin heat exchanger design using genetic algorithm", *Applied Thermal Engineering*, vol. 29, no. 14–15, pp. 2983–2989, 2009, ISSN: 1359-4311. DOI: http://dx.doi.org/10.1016/

j.applthermaleng.2009.03.009. [Online]. Available: http://www.sciencedirect.com/science/article/pii/S1359431109000945.

[38] N. Kovvali, *Theory and Applications of Gaussian Quadrature Methods*, ser. Synthesis digital library of engineering and computer science. Morgan & Claypool, 2011, ISBN: 9781608457533. [Online]. Available: https://books.google.com.co/books?id=uTCdW8L6i8sC.

[39] R. Shah, E. Subbarao, and R. Mashelkar, *Heat Transfer Equipment Design*, ser. Advanced study institute book. Taylor & Francis, 1988, ISBN: 9780891167297. [Online]. Available: https://books.google.com.co/books?id=eeN6GgF3v5MC.

[40] W. Kays and A. London, *Compact Heat Exchangers*. Krieger Publishing Company, 1984, ISBN: 9781575240602. [Online]. Available: https://books.google.com.co/books?id=A08qAQAAMAAJ.

3. STUDY OF GASKETED-PLATE HEAT EXCHANGER PERFORMANCE BASED ON ENERGY EFFICIENCY INDEXES

Juan Sebastián Rincón Tabares, Luis Perdomo-Hurtado*

*lperdomo@autonoma.edu.co

Departamento de Mecánica y producción, Universidad Autónoma de Manizales,

Antigua estación del ferrocarril, Manizales, Caldas, Colombia

Jose Luis Aragón Vera

Centro de Física Aplicada y Tecnología Avanzada, Universidad Nacional Autónoma de Mexico,

Boulevard Juriquilla 3001, Juriquilla, 76230 Queretaro, Mexico.

ABSTRACT

Gasketed-Plate heat exchangers have their main application in food processing industry when a liquid - liquid situation is required. The aim of this work is to show the behavior, by a performance analysis, using first and second thermodynamic laws on some operational configurations of feasible gasketed-plate heat exchangers. To reach it, 40 simulations were done using an adaptive damped secant shooting method to solve the distributed-U differential model proposed by Pinto and Gut. With simulation solutions, heat and exergy transfer effectiveness, dimensionless entropy generation, entropic potential loss and energy efficiency index were calculated when both fluids are above room temperature, below room temperature and almost one crossing room temperature. Main conclusion is that countercurrent configurations have better performance than parallel flow configurations due to influence of finite temperature difference in equipment and higher NTU are reached when fluids are above room temperature for same geometry.

3.1. Introduction

Heat exchangers (HX) are a group of devices that can transfer thermal energy from one fluid to another due to a temperature difference between them. Tubular, plate, and extended surface are the HX main groups classification based on construction geometries. Gasketed-Plate Heat Exchangers (PHX), also called plate and-frame heat exchangers, are equipment that belongs to the plate HX category [1].

A standard PHX consist on a group of corrugated plates, for heat exchanging improvement, which have strategically allocated gaskets that seals a channel between plates when they are compressed in a frame. Channels allow the fluids (that enter from the same or opposite sides of the equipment) to exchange heat, by co current or counter flow arrangement, though the plates. Due to this, PHX could reach a lot of different flow configurations including parallel, series, single, multi pass and their combinations, among others [2].

PHX can be found mainly in food and beverage processing industry but it can be found in pharmaceutical, rubber and petrochemical industries, and power plants, inter alia. [3]. Its compactness, high heat transfer coefficient, simple maintenance, low cost, and the easy adaptable heat transfer area through plate addition or plate dismounting , make PHX one of the most common device in all industries [4]. Additionally, PHX requires less bulky equipment with higher heat transfer surface compared to Shell and-Tube heat exchangers [5].

Correct sizing of a PHX is established depending on heat duty requirement and heat exchanger characteristics. Its flexibility and operative advantage contrast with the complexity to formulate a model for its steady flow behavior [6]. Wolf modeled PHXs as a coupled system of ordinary linear differential equations (ODE) in [7] and many solution methods have been proposed. Wolf [8], Zaleski [9], Settari & Venart [10], Zaleski & Klepacka [11], and Kandlikar & Shah [12] worked on the approximated solution to the system of ODEs, applying constant coefficients (not temperature dependent fluid properties) or simplified geometric/operative conditions.

Kandlikar & Shah [12] showed some guidelines for pass arrangements by effectiveness - NTU through different sets of design charts. They solved the linear ODEs coupled system, proposed by Wolf in [7], using the Gauss-Seidel iterative finite difference method. Their procedure produced results for 0 to 100 plates arrangements and six pass configuration. They settled that detailed design calculations are necessary to decide the best pass arrangement for an allowable pressure drop.

Zaleski & Klepacka [13], simulated around 150 different configurations for gasketed plate heat exchangers by solving the coupled ODEs system. They used fixed thermo physical fluid properties and an exponential function approximation for the temperature profiles. Zaleski & Klepacka took in account the plate number influence, fluids arrangement and port connection on average temperature difference, temperature effectiveness and logarithmic mean temperature difference. Zaleski & Klepacka's main conclusion was that couterflow configurations yields the highest effectiveness. Aditionally, Zaleski & Klepacka found some important relationships between geometrical, operational an thermal variables on PHX; for example, if the PHX channel number is large, heat transfer coefficient tends to decrease, and if both fluid pass number are equal or less than 2, parallel flow PHX are more efficient. It is important to highlight that In [13] all performance parameters were based on thermodynamics first law.

Pinto & Gut [2], modeled generalized PHX configurations by means of a system of ODEs, with constant coefficients, which allows an analytical solution. Then the results of the analytical solution were compared with the general temperature dependent solution. They concluded that their model is a useful tool to study the PHX performance and may be used to select the optimal configuration. In relation to that, the first step to rate an equipment is to model it to simulate the behavior of fluids under certain geometry and operating conditions. It is useful and common to use the results of certain simulations to perform calculation that can show additional and not obvious information of the HX how it is going to be shown next. Heat exchanger effectiveness, proposed by Kays & London [14], and exergy transfer effectiveness proposed by Wu et al. [15], are examples of rating parameters that expose hidden information that an only be discovered by additional calculations based on the quantity of energy and the quality of energy, respectively.

Qiao et al. [6] developed a generalized flow configurations PHX analysis model. Their model is capable of handling more than three fluids, flow maldistribution, single-phase, and two-phase flow. Quiao et al. model divided the PHX into discrete slices that were determined by successive substitution approach. They concluded that model's predicted results had matched their experiments within a 5% error in heat load and it is suitable for optimization context.

Sammeta et al. [4] used the results of CFD simulations over a 9 channel corrugated plate heat exchanger geometry to create $\varepsilon - NTU$ and $\theta - P$ performance charts, variating the fluids heat capacity ratio for a series-parallel and a series counterflow flow configurations. Their results show that series counterflow plate heat exchangers have the best performance and there is not heat capacity ratio influence on performance curves. They only analyzed first law parameters.

Khairul et al. [16] proposed an analytical - experimental procedure to measure exergy destruction and exergy transfer effectiveness on a corrugated plate heat exchanger. They used a counterflow PHX with hot water and multiple volume concentration cold metal oxide nanofluids solution to obtain the necessary data to calculate thermodynamic average temperature and exergy loses from both fluids. Khairul et al. noted that an increment on flow rate of the working fluid results in a higher pressure drop and pumping power. Additionally, cold fluid nanoparticles concentration increased the exergetic heat transfer effectiveness.

Wenterodt et al. [17] presented a second law analysis through irreversibilities and the entropic potential concept for an arbitrary energy transformation process. In the same manuscript, they applied the concept to a single-phase PHX with 45° "fish bone pattern" plates, where required data for theoretical analysis was obtained from a CFD simulation. Almost 2000 simulations results of a simplified model showed that an optimum value for minimum entropic potential loss or energy devaluation number could be reached for a certain Reynolds numbers.

Nilpueng et al. [18] presented some experimental results on water - water plate heat exchangers that worked over $25°C$, showing chevron angles, surface roughness, and working conditions impact on PHX thermo-hydraulic parameters, and thermal performance factor. They concluded that

optimal values of thermal performance factor were obtained for 30° chevron angle.

Recently, Zhang et al. [19] proposed a new criterion to grade energy efficiency on a PHX based on the overall heat transfer coefficient and pressure gradient ratio called Energy Efficiency Index (EEI). Zhang et al. stated that "EEI can quantitative test the performance of plate heat exchangers and hence can grade them in terms of energy efficiency", relating EEI directly with the first thermodynamics law but also concluded that it can match with second law of thermodynamics. PHX with $EEI \geq 206.12$ are high efficiency equipment and exchangers with $EEI \leq 176.35$ have low energy efficiency following their approach.

Tan et al. [20] studied the PHX performance using the Nusselt number and friction factor, changing chevron angle, corrugation aspect ratio and plate segments for laminar and turbulent flow. They found that increment in chevron angle and corrugation aspect ratio is a good way to enhance PHX performance but also the trade-off between heat transfer, and pressure drop could be considered in equipment design.

Real-life operating conditions are those working parameters (geometrical and thermo-hydraulic) based on realistic context which are used on equipment simulation to produce feasible results for industry [21]. Standing on this concept, room temperature and feasible pressure drop are two variables to take into account in HX rating and designing to represent a realistic context. Environmental temperature refers to the HX surrondings temperature. Martinaitis & Streckiene [22] analyzed HE-room thermal energy direction influence over exergy efficiency concluding that best performance could be reached designing away from room temperature. In addition, Martinaitis et al. [23] proposed a piecewise exergy efficiency function to overcome a variable room temperature condition for a HVAC (Heating, Ventilating and Air Conditioning) system, through Marmolejo & Gundersen [24] work. Martinaitis et al. concluded that their approach is suitable when reference environment temperature is above, across and below temperatures involved operation fluids in HVAC and that could be useful to obtain optimized designs when environment reference temperature changes during the operation.

On the other hand, pressure drop on PHX is a function of mass flow rate through channels; likewise mass flow rate is directly related to velocity inside them [2]. HX velocity have to be established maintaining a balance between, pressure drop, pumping power, fluid fouling, and pipelines erosion [1]. Based on these facts and fluid characteristics, there are recommended limits and optimal velocity values for PHX, based on actual operating conditions. Baek et al. [25] proposed a fouling removal procedure applying 1 m/s and 1.25 m/s to chilled water - air bubbles mix inside PHX channels. Bani & Peschel [26] exposed a study where velocity was increased from 0.30 m/s to 0.42 m/s on a CO_2 - water plate cooler to reduce fouling in plates. Changain et al. [27] proposed that there is not theoretical justification to clean PHX using 1.5 m/s for cleaning solution and stated that whey protein soil could be removed using the same solution at 0.175 m/s. Goode et al. [28] established that there were more fouling on PHX from condensed vapor on wort boiling system when velocity was 0.07 m/s than 0.14 m/s. Goode et al. stated too that higher flow velocity produces more efficient removal at the start of cleaning on shampoo fouling, using a velocity domain from 0.14 m/s to 0.47 m/s . Finally, experimental data obtained by China Standardization Committee on Boilers and Pressure Vessels, cited by Zhang et al. [19], proposed actual PHX velocity range from 0.1 m/s to 1.0 m/s.

This work aim consists in analyzing feasible PHX by particular first and second law performance indexes which take into account real operation velocities and environmental temperature effect. Indexes have been individually analyzed and in a group manner following the same thermal domain size (NTU) . In order to obtain accurate values for the gains and losses of energy for here selected efficiency indexes, the ODE set proposed by Gut & Pinto [2] has been solved using an stable and convergent approach. Stability and convergence are pretty important to future works on thermo-economic model optimizations. Thermodynamic and hydraulic fluid properties have been evaluated as a function of the internal temperature profile (main source of instabilities and convergence delays in the model solution) in order to understand indexes values through the different PHX configurations. Thermal size variation has been simulated adding and/or removing plates to PHX how it is carried out in a real industrial operation. Due to room temperature effect over the second law based indexes, different cases where fluid temperature profiles are above, below or, crossing room temperature have been studied. Current work is proposed as new tool

to select, evaluate or characterize new designs and/or installed single-phase PHXs at real operating and environmental conditions which affect the energy efficiency for these kind of important devices.

3.2. Methodology

3.2.1. PLATE HEAT EXCHANGER MODEL

The model presented by Gut & Pinto [2] has been selected to obtain the temperature distribution for each PHX fluid. Through this model, simulations can be carried out for generalized configurations as well as to solve a coupled system of differentials equations with constant or temperature-dependent coefficients. In addition to Gut & Pinto's model, fluid properties like heat capacity, thermal conductivity, density, viscosity, and thermal expansion coefficient have been calculated as a function of temperature inside the PHX using the empirical correlations of Yaws [29] and T-dependent coefficients or distributed-U model. The coupled set of ODEs for PHX can be written ,as a generalized form, as it is shown in Eq. (3-1).

$$\frac{dT_i}{dx} = \frac{s_i w \Phi U_{i-1}}{\dot{m}_i c_{P_i}} \left(T_{i-1} - T_i\right) + \frac{s_i w \Phi U_i}{\dot{m}_i c_{P_i}} \left(T_{i+1} - T_i\right) \tag{3-1}$$

Where T is fluid temperature, x is channel flow direction coordinate, s is channel flow direction parameter, w is effective plate width for heat exchanger, Φ is plate area enlargement factor, U is overall heat transfer coefficient, $\dot{m}$ is fluid mass flow rate and c_P is fluid specific heat at constant pressure; for each channel i between plates inside the heat exchanger.

Because T-dependent coefficients and fluid properties, the differential equations system solution must be done numerically, but taking in account that not all the necessary boundary conditions established are initial conditions. Consequently, an iterative "shooting method" has been proposed to solve the problem, following the approach present in [30]. The solutions scheme is presented in Fig. **3-1**. In addition, for each iteration, the new approximation have to be recalculated using a combination of different upgrades for the sake of algorithm speed and stability [30]. They include a one-step adaptive damped secant iteration, only using the numerical Jacobian matrix main diagonal obtained from previous approximation. Variable coefficients for the system of ODE includes

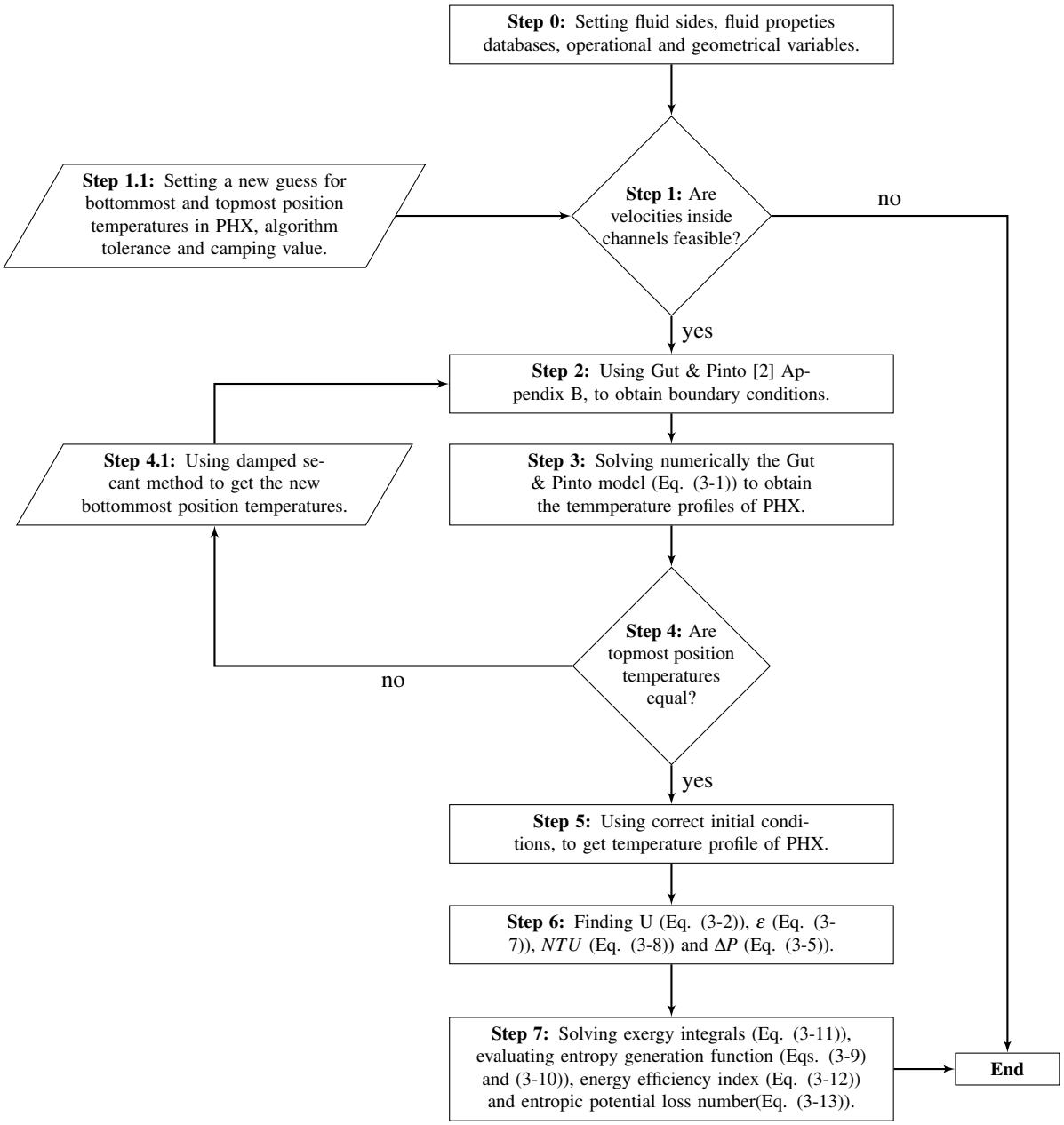

Figure 3-1: Shooting method algorithm

the global coefficient of heat transfer (U) for each control volume (two consecutive plates and the contained liquid between them) presented in Eq. (3-2).

$$U_i = \left(\frac{1}{h_i} + \frac{1}{h_{i+1}} + \frac{\delta_p}{k_p} + R_{fI} + R_{fII} \right)^{-1} \tag{3-2}$$

Where h is the convective heat transfer coefficient, δ_p is the thickness of metal plate, k_p is the

plate thermal conductivity and R are the fluid fouling factor for sides I and II. The theory of Martin [31] implies that momentum transfer is similar to heat transfer in plate heat exchangers, so empirical models presented in Eq. (3-3) for the Nusselt number (Nu) and Eq. (3-4) for the friction factor (f) have been taken from [3].

$$Nu = \frac{hD_h}{k} = 0.205 Pr^{1/3} \left(\frac{\bar{\mu}}{\mu_w}\right)^{1/6} \left(f \cdot Re_{D_h}^2 \sin(2\beta)\right)^{0.374} \tag{3-3}$$

$$\frac{1}{\sqrt{f}} = \frac{\cos(\beta)}{\left(0.045\tan(\beta) + 0.09\sin(\beta) + f_0/\cos(\beta)\right)^{1/2}} + \frac{1-\cos(\beta)}{\sqrt{3.8 f_1}} \tag{3-4}$$

Where D_h is the equivalent diameter of channel, k is the fluid thermal conductivity, Pr is the Prandtl number, $\bar{\mu}$ is the mean temperature viscosity, μ_w is the plate-wall temperature viscosity of the fluid, f is Fanning friction factor, Re_{D_h} is the Reynolds number , β is chevron corrugation inclination angle. The parameters f_0 and f_1 are proposed for Matin [31] that depend on the viscous flow regime inside each channel (turbulent or laminar flow).

The pressure drop expression, showed in Eq. (3-5) (extracted from [2]), takes into account three main mechanical energy losses: core heat exchanger fluid friction, movement between plates, and the gravitational effect (ΔP_g). In order to improve the friction factor calculation accuracy in the pressure drop analysis, Eq. (3-4) has been replaced by Eq. (3-6) which also was adapted from Elmaaty et al. [32] work. This empirical relation implies a dependence between plate friction factor, chevron angle, plate enlargement factor, Reynolds number and limit layer effect instead of Reynolds number and chevron angle in Eq. (3-4). For these calculi, all properties were computed at the average temperature of each fluid.

$$\Delta P = \left(\frac{2f\,(L+D_p)\,pG_c^2}{\bar{\rho} D_h}\right) + 1.4\left(p\frac{G_p^2}{2\bar{\rho}}\right) + \bar{\rho} g\,(L+D_p), \text{ for sides I and II} \tag{3-5}$$

$$f = \begin{cases} \left[\left(\frac{30.2}{Re_{D_h}}\right)^5 + \left(\frac{6.28}{Re_{D_h}^{0.5}}\right)^5\right]^{1/5} \cdot \left(\frac{\beta}{30}\right)^{0.83} \cdot \left(\frac{\bar{\mu}}{\mu_w}\right)^{-0.22} & Re_{D_h} < 1000 \\ A_M(\Phi) \cdot B_M(\Phi) \cdot Re_{D_h}^{C_M(\beta)} \cdot \left(\frac{\bar{\mu}}{\mu_w}\right)^{-0.22} & Re_{D_h} \geq 1000 \end{cases} \tag{3-6}$$

Where ΔP is the total pressure drop of the equipment, L is the plate length, D_p is the plate port diameter , p fluid pass number inside the plate heat exchanger, G_c is channel mass velocity, $\bar{\rho}$ is the average fluid density and g is the gravity acceleration. $A_M(\Phi)$, $B_M(\Phi)$ and $C_M(\beta)$ are empirically adjusted functions for Φ and β proposed by Elmaaty et al. [32], limited to chevron angle between 30 and 60 degrees that are the most common surface pattern for PHX.

Qiao et al. model [6] has been tested as an alternative to Gut & Pinto's model. For same single-phase application in this work, both models results have been compared and less than 1% outlet temperature difference has been found. Based on Eldeeb et al. [33] opinion, Gut & Pinto's model have been selected because its higher computational speed. When two-phase flow have to be simulated, it is required to change the selected model to Qiao et al. model because its features with this kind of fluids, impossible to simulate with Gut & Pinto's model.

3.2.2. PLATE HEAT EXCHANGER PERFORMANCE

Once a rigorous model to represent both fluid temperature profiles in a PHX has been obtained, a performance measurement is necessary to evaluate operational configurations. Energetic behavior of a HX based on thermodynamic first law could be understood as the quantity of energy that goes from hot to cold fluid limited by fluids properties, flow arrangement and equipment geometry [1]. On the other hand, second law energy analysis is directly related to irreversible processes inside HX when heat transfer at finite temperature differences, fluid mixing, phase change and/or fluid flow friction phenomena occurs. Those phenomena are geometry, fluid and flow arrangement dependent but environment dependent too. A change in those conditions cause an energy quality depression that reduces the amount of energy that could be used in heat transfer, when a HX is analyzed [3].

Many authors have proposed performance measurement parameters by what they interpreted as a performance of heat exchangers [24]. It is important to highlight that Bejan in [34], proposed a general criterion for rating heat exchangers performance called "Number of entropic production units" to quantify the inverse relation between ΔT and ΔP and irreversibility in a heat transfer

process. Additionally, Guo et al. in [35] stated that field synergy number, which relates velocity field and heat flow, could be helpful in Shell and-Tube heat exchanger optimization than other methods. Last authors in [36] proposed another performance parameter based on entransy dissipation concept that reflects the degree of irreversibility caused by flow imbalance. The entransy dissipation is a controversial concept that was analyzed by Kostic in [37] and disapproved by Bejan in [38] and Sekulic et al. in [39] as a useful tool on the study field.

According to this, five parameters have been chosen to quantify the performance of the plate heat exchangers: heat exchanger effectiveness, non-dimensional entropy generation, exergy transfer effectiveness, energy efficiency index and entropic potential loss number; based on Bejan's theories [34], [40] and judgments [38]. Selected parameters have been compared against the number of transfer units (NTU). It is important to highlight that changing NTU values is related with real applications of plates addition or remotion to the heat exchanger.

First, effectiveness (ε) or heat exchanger effectiveness, as well as NTU, are coupled in NTU-ε method that is a simplified way to design heat exchangers and measure it performance based on the relative quantity of energy that goes from hot to cold fluid compared to the enthalpy change rate of the fluid with less heat capacity [3], [41]. For the present analysis, ε and NTU have been calculated with Eq. (3-7) (adapted from [2]), and Eq. (3-8), taken from [3] and adapted to Pinto's model; respectively and for each PHX. Using Eq. (3-8), NTU was calculated for each plate and, according to Shah [3], the total NTU for the PHX is the sum of each plate NTU.

$$\varepsilon = \frac{\dot{m}\bar{c_p}\left|\theta_i - \theta_o\right|}{C_{\min}}, \text{ for sides I and II} \tag{3-7}$$

$$NTU = \frac{UA}{C_{\min}} = \frac{1}{C_{\min}}\int_A U dA = \frac{1}{C_{\min}}\int_0^L U\left(x\right) w \Phi dx \tag{3-8}$$

Where θ is the dimensionless standardized fluid temperature, $C_{\min}$ is the smallest heat capacity between fluids that limits the heat transfer and A is the effective plate heat transfer area. The charts presented in this document were obtained by changing the NTU by adding new plates to

the equipment. In this case, the minimum number of plates was fixed to 2 and the maximum was 60, restricted by the relation between damping and computational cost of algorithm to archive numerical convergence [30].

Shah [3] also proposed an expression to compute a dimensionless entropy generation (S^*) for heat exchangers . In the present work, this parameter is associated to the sum of three phenomena that produces irreversibilities in the PHX, they are the finite temperature difference (FDT) between fluids and the fluid friction (FF) inside the substances and within the fluid and the equipment caused by the viscosity of hot and cold fluids[3]. So expressions in Eq. (3-9) and Eq. (3-10), have been used to calculate this dimensionless parameter, taking into account that the water has been treated as a non compressible liquid.

$$\frac{\dot{S}_{FF}}{C_{\max}} = S^*_{FF} = \frac{\dot{m}\Delta P}{\bar{\rho} C_{\max}} \cdot \frac{\ln\left(T_o/T_i\right)}{T_o - T_i}, \text{ for sides I and II} \tag{3-9}$$

$$\begin{aligned} &\tfrac{\dot{S}_{FTD}}{C_{\max}} = S^*_{FTD} = \\ &= \tfrac{C_{\min}}{C_{\max}} \ln\left[1 + \varepsilon\left(\left(\tfrac{T_{II,i}}{T_{I,i}}\right) - 1\right)\right] + \ln\left[1 + \tfrac{C_{\min}}{C_{\max}}\varepsilon\left(\left(\tfrac{T_{I,i}}{T_{II,i}}\right) - 1\right)\right] \end{aligned} \tag{3-10}$$

Where $\dot{S}$ is the entropy generated by irrevesibilities, $C_{\max}$ is the largest heat capacity between fluids and the * means dimensionless.

Now exergy transfer effectiveness (ε_e) means the relation between exergy actually transferred to objective fluid against its theoretical maximum [41], based in the theory developed by Wu [15]. Its application to the current work have required the use of the correct definition in each situation as has been described by Marmolejo [24] and Martinaitis et al. [23]. Those situations have been coupled to the selection of a room temperature, which caused different behaviors if the temperature profiles were all above, all below or any of them crossing this room temperature. Barron [42] stated that there is always thermal energy exchange between equipment and the environment that degrades the HE performance, specially on T_∞ HE. Changes in reference environment leads to changes on energy and exergy transfer direction as stated by Martinaitis et al. [23]. In addition, Martinaitis & Streckienke concluded in [22] that HE that works near room temperature, tend to

have low exergy efficiency values.

Because room temperature cases, the definition used to calculate the exergy change in the first two cases is presented in Eq. (3-11), and for the third case, the expressions $1-\frac{T_\infty}{T}$ and $T-T_\infty$, in parenthesis, changes their sign as was proposed in [24]. Additionally, due to dependence on gravitational pressure drop used to calculate the exergy change, the maximum exergy change took in account this component on the pressure drop for all simulations done.

$$\varepsilon_e = \frac{\int_{T_i}^{T_o} \dot{m} c_P \left(1-\frac{T_\infty}{T}\right) dT + \int_{P_i}^{P_o} \dot{m} \left[v-(T-T_\infty)\left(\frac{\partial v}{\partial T}\right)_P\right] dP}{\int_{Tci \text{ or } Thi}^{Thi \text{ or } Tci} \dot{m} c_P \left(1-\frac{T_\infty}{T}\right) dT + \int_{P_i}^{P_i+\Delta P_g} \dot{m} \left[v-(T-T_\infty)\left(\frac{\partial v}{\partial T}\right)_P\right] dP} \tag{3-11}$$

Where T_∞ is the room temperature and v is the specific volume.

Another parameter is the Energy Efficiency Index (EEI), recently proposed by Zhang et al. [19]. This value was specifically created to measure the performance in single phase flow plate heat exchangers. EEI was defined as it appears in Eq. (3-12) and its meaning is related directly with performance of PHX in terms of energy efficiency [19], but is in a good agreement with the second law of thermodynamics too. Their approach shows a connection between energy losses related to fluid friction in each fluid, the equipment geometry and the energy transfer potential involving all heat transfer phenomena from hot to the cold fluid. Here, the overall heat transfer coefficient used was the mean of all distributed heat transfer coefficients in Gut & Pinto's model.

$$EEI = \frac{U}{\left(\omega_I \frac{\Delta P_I}{L} + \omega_{II} \frac{\Delta P_{II}}{L}\right)^n} \tag{3-12}$$

Where ω is a weight coefficient for pressure drop - plate length rate in each side of the PHX and n is a factor that characterizes heat transfer process PHX in Zhang et al. base line database. Following the recommendation of [19], n have been set to 0.31 based on less fluctuation criterion against channel flow velocity stated by Zhang et al.. Finally, the last parameter has been computed to get an entire spectrum of the equipment performance. This value was the Entropic Potential

Loss Number (N_{EPL}) proposed by Wenterodt et al. [17] that is presented in Eq. (3-13). This index shows how bad a process or a component might be, connecting it with the energy quality reduction given by the entropy generated during the equipment operation [17]. Moreover, its value depicts the fraction of entropy discharged to the ambient when the heat transfer process is done.

$$N_{EPL} = \frac{\dot{S}_{gen} T_{\infty}}{\dot{Q}} \tag{3-13}$$

Where $\dot{S}_{gen}$ and $\dot{Q}$ are total entropy generation and heat transferred from hot to cold fluid, respectively.

3.2.3. OPERATION CONDITIONS

Fixed operative conditions, used in this work simulations, are shown in Table **3-1**. These conditions are similar to those used in [2] but both fluids are water instead. As aforementioned in section 3.1, the three cases concerning environmental temperature effect have been considered for both fluid inlet temperatures and they are: all above (a) or below (b) room temperature, and one or both fluid temperatures crossing it (c) at some point in the PHX. To ensure the heat transfer process and to study (a), (b), and (c) cases, inlet fluid temperature difference and three different cold fluid inlet temperatures were fixed using values of $20K$, $30°C$, $2°C$, and $15°C$ respectively.

Table 3-1: Operative conditions

	Fluid	$\dot{\mathbf{m}}$ $[kg/s]$	$(\mathbf{R_f})$ $[m^2K/W]$
Side I	Hot water	1.30	1.7×10^{-6}
Side II	Cold water	1.30	1.7×10^{-6}

Equipment geometry used in simulations is shown in table **3-2**. This geometric parameter set is similar to used by Gut & Pinto in [2] but with the commertial characteristics recommended for PHX in [19] and diagonal flow channels.

Zaleski & Klepacka [13], after observing PHX behavior, found that two-pass/two-pass-flow showed better performance than other multiple-pass configuration. It has been chosen as starting

Table 3-2: Plates characteristics

Parameter	**L** $[cm]$	**w** $[cm]$	**b** $[mm]$	**Dp** $[cm]$	β $[^\circ]$	Φ	δ_p $[mm]$	k_p $[W/mK]$
Value	74	23.6	2.7	5.9	45	1.17	0.7	17

point to analyze cold fluid inlet port impact on PHX performance. Potential inlet ports are show in Fig. **3-2** where four positions are: for parallel flow, next to hot fluid entrance ($\phi = 1$), at the same side but in the other end of the frame ($\phi = 2$) and, in counterflow, in front of ($\phi = 3$) and diagonal ($\phi = 4$) to hot fluid entrance in the PHX.

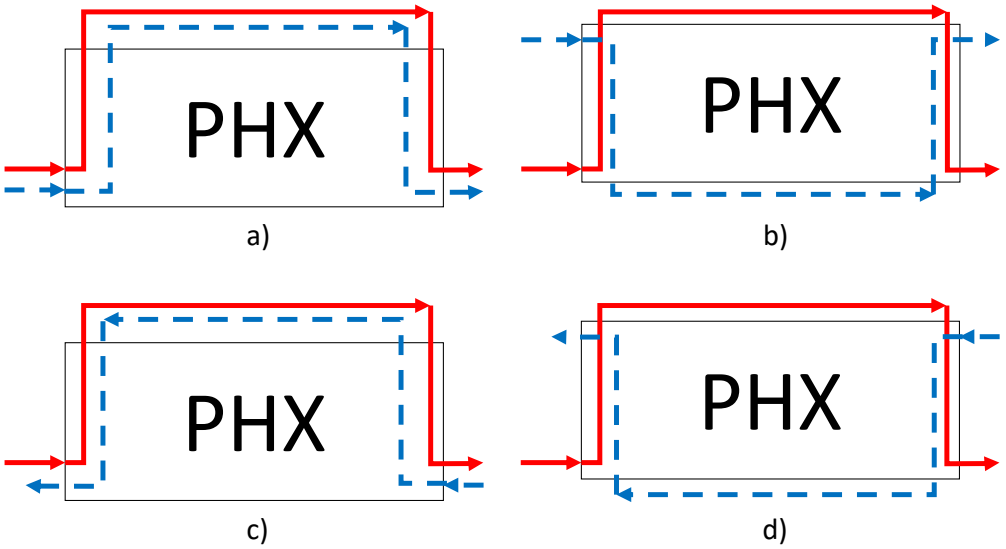

Figure 3-2: Fluids connection port and route in plate heat exchanger: a) $\phi = 1$, b) $\phi = 2$, c) $\phi = 3$ d) $\phi = 4$. Solid line: hot fluid, dashed line: cold fluid.

Simulation algorithm (Fig. **3-1**) includes a condition to obtain feasible configurations. This condition is mean velocity value inside each channel, calculated at inlet conditions of each fluid. Velocity limits were fixed from 0.1 m/s to 1 m/s according to [19]. Condition reason has been the unreal pressure drop triggered by high mass flow rate, related to speeds higher than the upper limit and low heat transfer coefficients at lower speeds [1].

3.3. Results

How it was said before, it have been analyzed cold fluid connection port and room temperature influence on industrial PHX first and second law performance. Typically, HX behavior is discussed based on NTU that is influenced by geometry, heat transfer, and operating conditions (Eq. (3-8)). However, for fixed operating conditions and uncontrollable U, NTU is entirely ruled by geometry changes. Fig. **3-3** (a) have been created to show the relationship between actual geometry change and NTU. Fig. **3-3** (a) chart is crucial to turn NTU in an actual industrial easy controllable discrete PHX parameter.

3.3.1. HEAT EXCHANGER EFFECTIVENESS-NTU

It is possible to realize that, for all indexes, simulated under the same geometric parameters, the equipment working below T_∞ handles the lowest NTU, against applications that are above or crossing room temperature. Those corresponding to the equipment with the largest thermal size are established for applications above room temperature. Hence, how it was shown in [3], geometric equipment equality does not necessarily represent the same NTU. Therefore, Fig. **3-3** (b) has been obtained overlaying room temperature cases curves that does not have same domain, as commented before and as a result of ε external variables independence, for instance, room temperature.

For the particular situation of $\phi = 3$, the fluid comes out with the 80 percent of the maximum theoretical energy transfer it could reach, according to the first law of thermodynamics. In addition, this is the equipment with the best performance in this parameter, with a tendency to improve as soon as the thermal size of the equipment is increased (increasing the heat transfer area increases the overall coefficient of heat transfer, see Fig. **3-3** (b). This is reflected in a better heat transfer from the hot fluid to the cold under the operating conditions.

As seen in Fig. **3-3** (b) that $\phi = 1$ configuration reached its theoretical asymptotic point in $NTU = 2$, which means that, although its thermal size increases, the performance of the first law cannot improve beyond a value close to $\varepsilon = 0.5$. It contrasts to $\phi = 3$ and $\phi = 4$ behavior

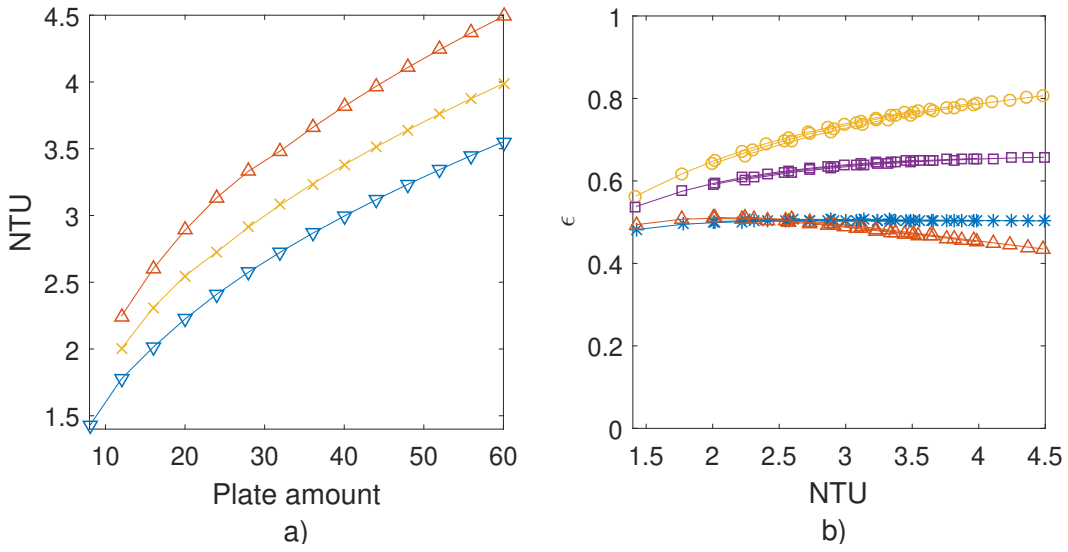

Figure 3-3: a) Plate amount in heat exchanger vs. NTU. Above room temperature (upward triangle), Crossing room temperature (cross), below room temperature (downward triangle)
b) Effectiveness vs. NTU. $\phi = 1$ (star), $\phi = 2$ (triangle), $\phi = 3$ (circle), $\phi = 4$ (square)

.

because they tend to increase in effectiveness for values larger than $NTU = 2$ (in a higher rate for $\phi = 3$ than for $\phi = 4$ connection) or, on the contrary, it tends to decrease as the $\phi = 2$ configuration.

$\phi = 2$ configuration reaches its maximum performance for small equipment when $NTU = 2$ (see Fig. **3-3** (b)). From that point, there is an ε tendency to decrease with plate heat exchange size increase without finding the asymptotic behavior indicated by [1], [3]. As seen in Fig. **3-2** (b), this behavior is directly related to parallel flow pattern and ε dependence on temperature difference (see Eq. (3-7)) that decreases though PHX.

3.3.2. EXERGY TRANSFER EFFECTIVENESS-NTU

As shown in Eq. (3-11), exergy transfer effectiveness is highly dependent on T_∞. It must be highlighted that exergy destruction, associated with heat transfer and irreversibilities from or through environment could be useful or useless depending on the PHX aim. If there is a energy increasing requirement for a fluid, energy quality loss, could be beneficial to reach equipment objective [3],

otherwise it is futile.

This index is presented in Fig. **3-4** for hot fluid and Fig. **3-5** for cold fluid. It has a high dependence on the direction in which the heat is transferred between the fluids, and between the fluids and the environment, and represents the amount of useful energy of each fluid with respect to its reference environment [15], [24]. This is noted in the reversal of the location of the curves of effectiveness of the hot fluid when both are above room temperature (Fig. **3-4** (a)) and those representing the cold fluid when both substances are below room temperature (Fig. **3-5** (b)). This is a normal behavior proposed by [24] and depends on the gap between the fluid inside the PHX and the reference state.

For any of the cases represented in Fig. **3-4** and Fig. **3-5**, the configuration with $\phi = 3$ connection, is the one that shows the best performance either with the hot or cold fluid and so the one that most exergy transmits to the target medium. In addition, increasing the size of the equipment positively affects its performance according to [15] definition.

The case where both fluids are above the ambient temperature (Fig. **3-4** (a) and Fig. **3-5** (a)), is the one that presents the most dissimilar behaviors between the possible types of connection. $\phi = 1$ and $\phi = 4$ configurations reach the asymptotic value of operation in the proposed domain for both the hot fluid as for the cold. On the other hand, when the fluids are both below the ambient temperature (as seen in Fig. **3-4** (b) and Fig. **3-5** (b)), it can be highlighted that the small equipment performance under this parameter is very similar but they changes a lot with area increment. Performance equality becomes much more noticeable, when any of the fluids crosses the temperature of the reference environment (as seen in Fig. **3-4** (c) and Fig. **3-5** (c)), for a greater part of the domain, except for the equipment with $\phi = 3$ connection, which has a marked tendency to improvement.

Again, under the qualification of this parameter (based on thermodynamics second law), it is the parallel flow connection with the $\phi = 2$ port the one that has the worst performance. For it, the quality of the energy is seriously degraded when the size is enhanced (as seen in Fig. **3-4** (a) and

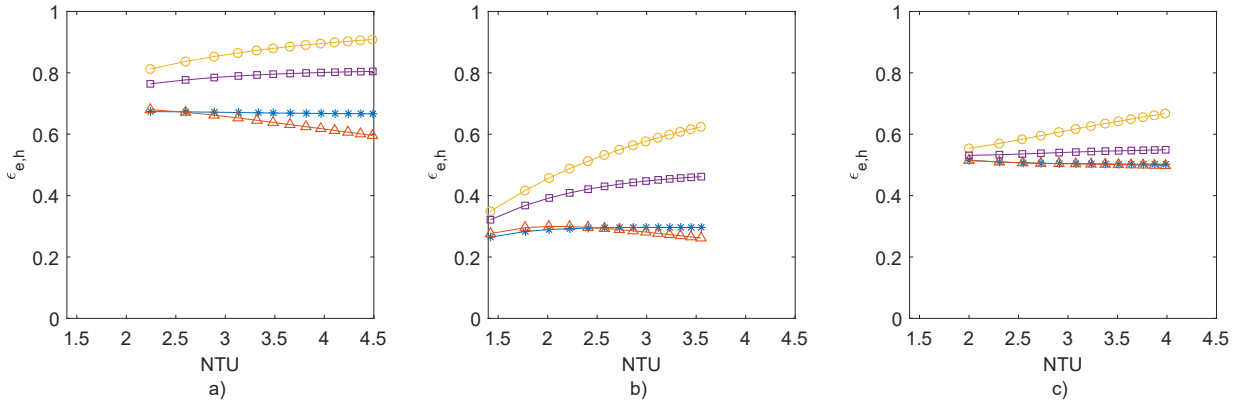

Figure 3-4: Hot fluid ε_e vs. NTU for: a) both fluids above room temperature, b) both fluids below room temperature, c) almost one fluid crossing room temperature. $\phi = 1$ (star), $\phi = 2$ (triangle), $\phi = 3$ (circle), $\phi = 4$ (square)

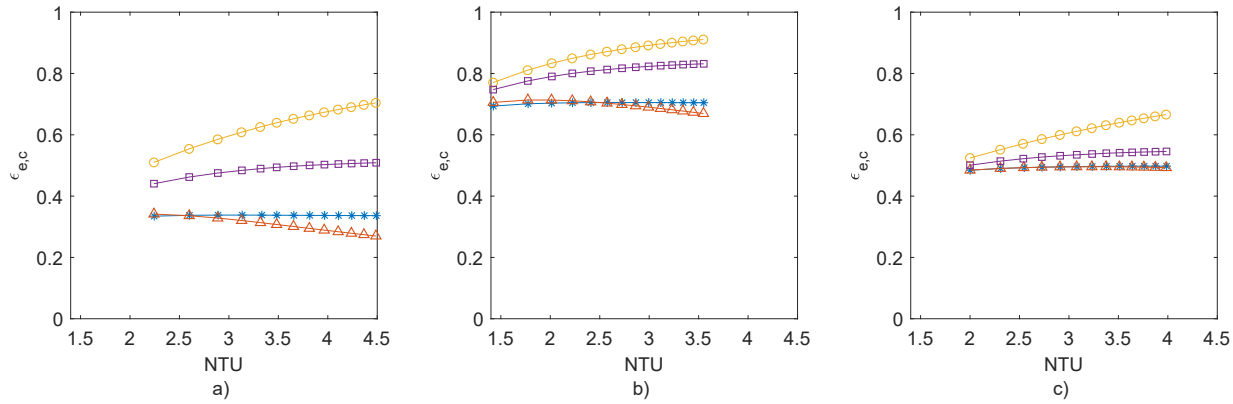

Figure 3-5: Cold fluid ε_e vs. NTU for: a) both fluids above room temperature, b) both fluids below room temperature, c) almost one fluid crossing room temperature. $\phi = 1$ (star), $\phi = 2$ (triangle), $\phi = 3$ (circle), $\phi = 4$ (square).

Fig. **3-5** (a)). In addition to this, its greatest performance is achieved in smaller equipment (NTU around 2.0 in Fig. **3-4** (b) and Fig. **3-5** (b)) and from there a downward trend is shown, with respect to the non-dimensional size of heat transfer.

The situation, in which the ambient temperature is crossed, greatly influences the performance of the equipment, as seen in the figures **3-4** (c) and **3-5** (c). This is derived from Newtonian fluids low viscosity at room temperature that indeed impacts on pressure drop values. Just in $\phi = 3$ case, it is possible to improve the exergy transfer to the target fluid and only under the premise of feasibility in the handling of relatively large equipment area. It is proposed to apply the plate and frame heat exchangers in situations where both fluids are above or below the ambient temperature.

3.3.3. DIMENSIONLESS ENTROPY GENERATION-NTU

As it was shown in the Fig. **3-6** , the entropy generation trend is lower as the thermal size of the equipment becomes greater; phenomenon that is related to lower speeds through the flow channels, parameter directly associated with the pressure drop, as shown by the Eq. (3-9).

The finite difference of temperature component is relevant in the equipment second law performance. As it is shown in the section 3.2.3, operating conditions were established with a maximum temperature difference between fluids of $20K$, regardless of the situation to be analyzed. However, depending on the type of connection selected, this difference occurs at the inlet of PHX in $\phi = 1$ and $\phi = 2$ cases, with a low reduction rate for $\phi = 2$ about the increase in the size of the equipment, as seen on figures **3-6** (a) and **3-6** (c). For $\phi = 3$ configuration, thermal shock is the least of all, since the temperature difference of $20K$ does not occur for the steady state operation, because fluids are countercurrent and have already traveled a certain distance inside the heat exchanger as seen in Fig. **3-2** (c). For this reason, dimensionless entropy generation is the lowest for $\phi = 3$. In the current liquid-liquid application pressure drops has its greatest influence when high channel velocity equipment are analyzed. When S^* is measured on that PHX, they have greater generation rate than those with the lower velocities, but it does not greatly affects fluid properties. On the other hand, when multiphase or gas applications are required, pressure drop will affect the fluid properties additionally and it have to be taken into account in a rigorous way.

Equipment with the lowest fluid temperature have the greatest capacity of entropy generation compared to those with higher temperatures because, as it is seen in the Fig. **3-6** (b), they are those that present higher values of this parameter, phenomenon associated with higher viscosities and densities that make more difficult the pass through channels and that lead to further pressure drops in the equipment plus heat transfer to surroundings. It is also possible to see in Fig. **3-6** (b) that the location of the cold fluid inlet connection is irrelevant in the smaller feasible equipment, since as shown, the curves start from the same point in a value of NTU close to 1.4 and they have a small difference up to the value of 1.7. It is a similar behavior presented in Fig. **3-4** (b) and

Fig. **3-5** (b) when cold fluid ε_e is analyzed, but not as marked as with S^*. In contrast to it, the analysis based on N_{EPL} shows a dissimilar behavior between port connection in all NTU domain regardless the temperature case, as can be seen in Fig. **3-8**.

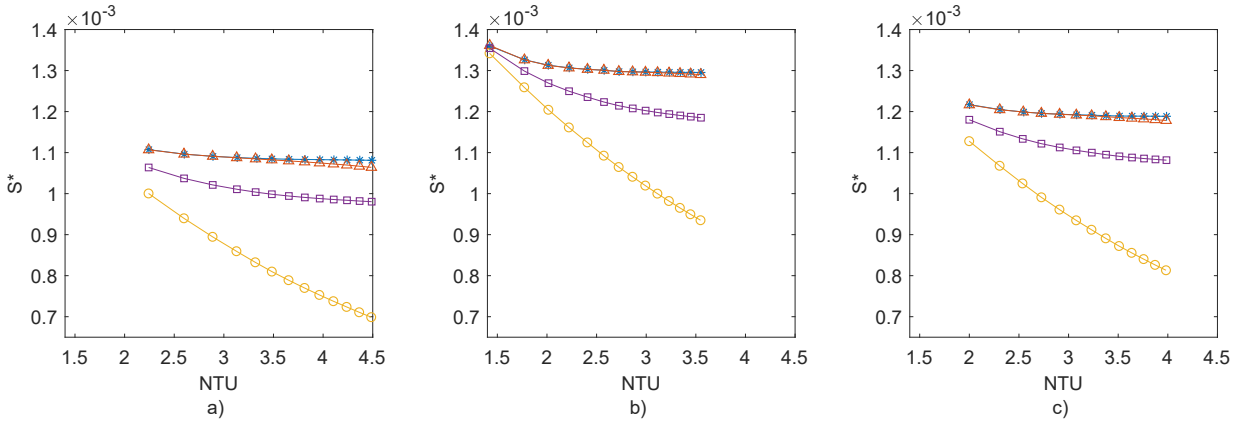

Figure 3-6: Dimensionless entropy generation vs. NTU for: a) both fluids above room temperature, b) both fluids below room temperature, c) almost one fluid crossing room temperature. $\phi = 1$ (star), $\phi = 2$ (triangle), $\phi = 3$ (circle), $\phi = 4$ (square).

Again, it is $\phi = 3$ equipment that presents the best performance and it can be improved by adding plates to the exchanger for the three situations analyzed in Fig. **3-6**. Therefore, this equipment has the lowest degeneration in the quality of energy that is transmitted (heat) and is added (pumping power) to both fluids for its passage through the heat exchanger. In contrast, $\phi = 1$ and $\phi = 2$ configurations have the worst performance among the possible types of connection for the equipment. Unlike other indicators, PHX with $\phi = 2$ connection, at least when both fluids are above room temperature, have a slight tendency to improve its operation as the thermal size of the equipment increases (see Fig. **3-6** (a)).

3.3.4. ENERGY EFFICIENCY INDEX-NTU

In the analysis of this parameter, it have to be highlighted that there is a lack of influence related to the location of the cold fluid inlet connection on EEI but it is influenced by room temperature cases, as expected by U and ΔP dependence on fixed geometric and operative parameters. As it is shown in the Fig. **3-7**, using EEI it is possible to see that the smallest heat exchangers have a better relationship between their capability to transfer heat and its pressure drop (as seen in the left side of Fig. **3-7**). This indicates that they transfer the energy better from one fluid to another,

despite having the greatest pressure drops due to the high velocity of the fluid passing through the channels in contrast to those of greater thermal size. This agrees with what is stated by [1], because with greater speed there is greater turbulence and heat transfer is better. Room temperature cases influence is directly related to T-dependent fluid properties because U and ΔP are a function of them.

According to [19], all configurations simulated are in the group of low energy efficiency plate heat exchangers due to $EEI < 176.35$. Energy Efficiency Index has a downward trend as the size of the equipment increases as it appear in Fig. **3-7**. In contrast to what was said by [19], in the present work, at higher speed (that leads higher turbulence and Reynolds number), it has been found the best index values, mainly related to lower pressure drop in little equipment. In addition, the lowest exergy transfer effectiveness for counterflow configurations and, the best ε_e for parallel flow configurations, associated, moreover the pressure drop, to higher or lower heat transfer coefficient, respectively have been found for the best EEI values. As it is seen in Fig. **3-7**, higher temperature equipment have the best performance. It is a result from the less pressure drop inside those PHX that have warmer fluids (with less viscosity and density) through their channels.

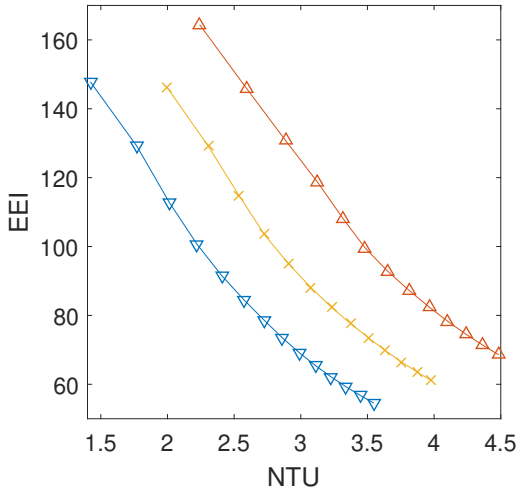

Figure 3-7: T_∞ influence on EEI. BAbove room temperature (upward triangle), Crossing room temperature (cross), below room temperature (downward triangle).

It is understood that heat transfer and pressure drop have to be weighted up in order to balance

the inverse proportionality of heat transfer rate and dissipation in HX but EEI is not necessary a good indicator for HX design. Its physical formulation only takes into account a first law criteria due to it is based on Nusselt number and friction factor ratio. Despite Zhang et al. [19] conclude that EEI shows a good agreement with the second law, it is clear that Eq. (3-12) only relates first law criteria and n exponent cannot be physically related with second law. How it was mentioned, Zhang et al. chose n exponent by trial and error (instead of an optimization approach), reaching a 0.31 value which leads a low variance (due to velocity fluctuation) respect to an "efficient" average value of EEI. The correlation between EEI and exergy efficiency, presented in [19], do not follow a quantitative approach, just a highly fortuitous numerical coincidence.

3.3.5. ENTROPIC POTENTIAL LOSS NUMBER-NTU

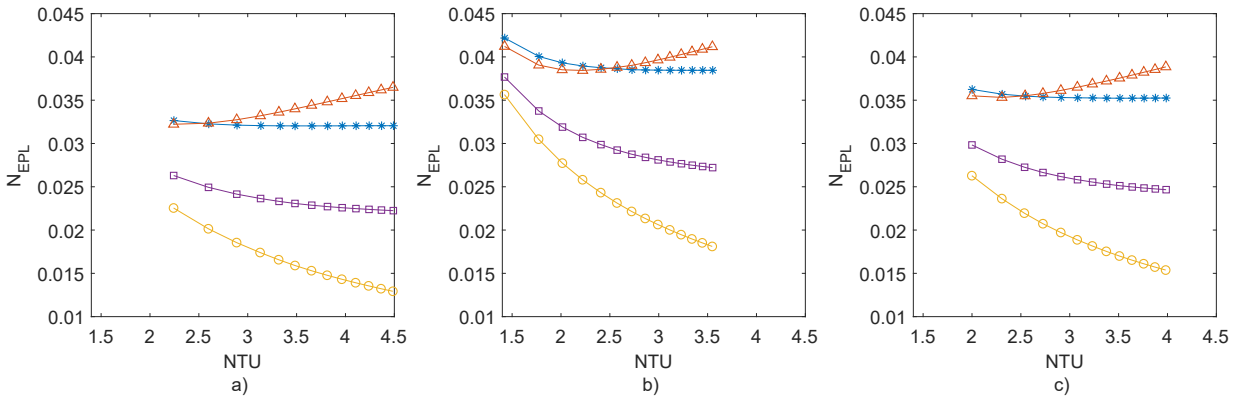

Figure 3-8: N_{EPL} vs. NTU for: a) both fluids above room temperature, b) both fluids below room temperature, c) almost one fluid crossing room temperature. $\phi = 1$ (star), $\phi = 2$ (triangle), $\phi = 3$ (circle), $\phi = 4$ (square).

As it can be seen in Fig. **3-8** (b), heat transfer processes that can most discharge entropy to the environment are those that are made below the ambient temperature. This may be due to pressure drop becomes more noticeable when the viscosities and densities are lower and heat goes from environment to them due to temperature difference between it and fluids inside PHX. Entropic potential is also increased by heat exchange process and direction between cold fluids and the surroundings of PHX, as exposed in second thermodynamics law.

For all temperature cases measured with N_{epl}, the $\phi = 3$ equipment tend to generate the lowest amount of entropy when the heat transfer is done. This is because the thermal shock between the substances is the least compared to $\phi = 1$, $\phi = 2$ and $\phi = 4$ equipment connection, as was

exposed in Fig. **3-2**. It is also necessary to affirm that higher thermal size, leads to reduction in Entropic Potential Loss Number related to better equipment performance.

For the three simulated cases, the connection represented by $\phi = 2$ is the worst and has its value of minimum entropy loss in small equipment ($NTU = 2.2$), which means that this type of connection is not recommended for equipment with many plates. For these devices, it would be losing to the environment more than 3.2% of the heat that will be transmitted between the working fluids.

In the case of the $\phi = 1$ connection, in all situations analyzed, it reaches an asymptotic value of entropy generation potential by heat transfer of 3.2% for both fluids above room temperature (Fig. **3-8** (a)), 3.9% for both fluids below room temperature (Fig. **3-8** (b)) and 3.5% for some of the fluids crossing the room temperature (Fig. **3-8** (c)). This implies that adding plates to the heat exchanger,does not change the relationship between the entropy released to the environment and heat transferred, in PHX where $NTU \geq 3.5$.

Based on all indexes, there is better first and second law performance in counterflow configurations ($\phi = 3$ and $\phi = 4$ cold fluid connection port) than parallel flow configurations ($\phi = 1$ and $\phi = 2$ cold fluid connection port). $\phi = 3$ configuration can exchange more heat in a less irreversible way, generates less entropy and tend to expel less to entropy to surroundings when energy movement is done, that represents the best energy use between port options. On the other hand, $\phi = 2$ has the worst performance plus there is not improvement while heat transfer area is increased. Authors encourage avoiding its use when it is possible. According to room temperature cases, energy quality is better preserved when both fluid are above room temperature. It is supported by higher thermal sizes, higher exergy transfer between fluid and less lost heat to surroundings. Nevertheless, PHX goal must be considered to act on PHX performance improvement because surroundings are an uncontrollable system that could be used as an extra energy source or sink.

3.4. Conclusions

A performance analysis of first and second thermodynamic laws was done over 40 configurations of plate heat exchangers. By both laws analysis is concluded that counterflow $\phi = 3$ connection is the best configuration for a plate heat exchanger due to its performance against other kind of connection. The worst plate heat exchangers are those that have $\phi = 2$ connection port because they generates the greatest irrversibilities from finite temperature difference.

Based on heat transfer effectiveness definition, $\phi = 2$ cold fluid inlet port configuration equipment have an uncommon behavior because the does not have an asymptotic value when the thermal size of the equipment becomes bigger. Instead, they have a maximum performance and after that, effectiveness tend to decrease.

Departing from exergy transfer effectiveness results, an asymptotic value was reached for $\phi = 1$, $\phi = 2$ and $\phi = 4$ cold fluid inlet port configuration equipment for both fluid when, almost one fluid, crosses the room temperature. In contrast, for $\phi = 3$ configuration ε_e increase it value in the same situation. Exergy efficiency tends to decrease for $\phi = 2$ in the remain 2 cases.

For PHX with the lowest NTU and below room temperature, does not have different dimensionless entropy generation parameter. When equipment get bigger, there are strong difference between parallel ($\phi = 3$ and $\phi = 4$) and counterflow ($\phi = 1$ and $\phi = 2$) configurations as the same way than over and crossing room temperature.

Energy efficiency index is not affected by cold fluid port location, but it is sensible to temperature. Plate heat exchangers with higher temperature can transfer heat in a better way and have the lowest pressure drop.

Finally, plate and frame heat exchangers working below T_∞ have the highest chance to discharge entropy to environment. In those equipment configurations, fluid friction component for pressure drop and the direction of heat transfer between environment and fluid have a greater impact when

the heat transfer process is done.

The exposed work is a guide that can be used as a tool to select the operating and installation conditions for single-phase PHX. It also could be used to choice PHX configurations according to environmental conditions of any place. It is outside of the scope the current work to analyze performance on multiphase heat exchanger due to the limitations of Gut & Pinto's model but with a powerful tool, it could be done with a similar procedure. Moreover, this work have only used an energetic first and second thermodynamics law performance approach, without including the cost performance for manufacturing, operation and/or maintenance of PHX, that could be computed based on the results of the simulations and adding cost indexes, as proposed by Bejan [40].

3.5. Nomenclature

T	, Temperature,	$[K]$.
x	, Channel flow direction coordinate,	$[m]$.
s	, Channel flow direction parameter,	dimensionless.
w	, Effective plate width for heat exchanger,	$[m]$.
U	, Overall heat transfer coefficient,	$[W/m^2K]$.
$\dot{m}$	, Mass flow rate,	$[kg/s]$.
c	, Specific heat,	$[J/kgK]$.
h	, Convective heat transfer coefficient,	$[W/m^2K]$.
k_p	, Plate thermal conductivity,	$[W/mK]$.
R_f	, Fouling Factor,	$[m^2K/W]$.
Nu	, Nusselt number,	dimensionless.
f	, Fanning friction factor,	dimensionless.
D_h	, Equivalent diameter of channel,	$[m]$.
k	, Fluid thermal conductivity,	$[W/mk]$.
Pr	, Prandtl number,	dimensionless.
Re	, Reynolds number,	dimensionless.
f_0	, Martin's parameter 0 for friction factor,	dimensionless.
f_1	, Martin's parameter 1 for friction factor,	dimensionless.
P	, Pressure,	$[Pa]$.
L	, Plate length,	$[m]$.
D_p	, Port diameter of plate,	$[m]$.
p	, Number of passes of each fluid inside the plate heat exchanger,	dimensionless.
G_c	, Channel mass velocity,	$[kg/m^2s]$.
g	, Gravity acceleration,	$[m/s^2]$.
A_M	, Empirically adjusted Φ function by Muley for f,	dimensionless.
B_M	, Empirically adjusted Φ function by Muley for f,	dimensionless.
C_M	, Empirically adjusted β function by Muley for f,	dimensionless.
C	, Heat capacity,	$[W/K]$.

A , Effective plate heat transfer area, $[m^2]$.

S , Entropy, $[J/K]$.

$\dot{S}$, Entropy rate, $[W/K]$.

$\dot{Q}$, Heat transfer rate, $[W]$.

b , Channel average thickness, $[m]$.

v , Specific volume, $[m^3/kg]$.

3.5.1. SYMBOLS

Φ , Plate area enlargement factor, dimensionless.

δ_p , Thickness of metal plate, $[m]$.

μ , Fluid viscosity, $[Pa \cdot s]$.

β , Plate chevron corrugation inclination angle, $[Degrees]$.

Δ , Increment / decrement,

ρ , Fluid density, $[kg/m^3]$.

ε , Heat exchanger effectiveness, dimensionless.

θ , Standardized fluid temperature, dimensionless.

ε_e , Exergy transfer effectiveness, dimensionless.

ϑ , Inlet temperature ratio, dimensionless.

ω , Weight coefficient for pressure drop - plate length rate, dimensionless.

ϕ , Cold fluid inlet port connection.

3.5.2. SUPERSCRIPTS

* , Dimensionless.

n , Zhang et al.'s factor for heat transfer process in PHX.

3.5.3. SUBSCRIPTS

i , Plate heat exchanger channel, inlet .

p , Plate, port.

I , Hot side.

II , Cold side.

h , Hydraulic.

w , Wall.

o , Outlet.

c , Channel.

h , Hot fluid.

c , Cold fluid.

g , Gravity associated.

∞ , Room or ambient.

gen , Generation.

3.5.4. ABBREVIATIONS

HE , Heat Exchanger.

PHX , Gasketed-Plate (and frame) Heat Exchanger.

NTU , Number of Transfer Units.

FF , Fluid friction.

FTD , Finite Temperature Difference.

EEI , Energy Efficiency Index.

EPL , Entropic Potential Loss.

ODE , Ordinary Differential equation.

CFD , Computational Fluid Dynamics.

$HVAC$, Heating, Ventilating and Air Conditioning.

Bibliography

[1] S. Kakac, H. Liu, and A. Pramuanjaroenkij, *Heat exchangers: selection, rating, and thermal design*. CRC press, 2012, ISBN: 1-4398-4990-0.

[2] J. A. W. Gut and J. M. Pinto, "Modeling of plate heat exchangers with generalized configurations", *International Journal of Heat and Mass Transfer*, vol. 46, no. 14, pp. 2571–2585, Jul. 2003, ISSN: 0017-9310. DOI: 10.1016/S0017-9310(03)00040-1. [Online]. Available: http://www.sciencedirect.com/science/article/pii/S0017931003000401.

[3] R. K. Shah and D. P. Sekulic, *Fundamentals of Heat Exchanger Design*. John Wiley & Sons, Aug. 11, 2003, 978 pp., ISBN: 978-0-471-32171-2.

[4] H. Sammeta, K. Ponnusamy, M. Majid, and K. Dheenathayalan, "Effectiveness charts for counter flow corrugated plate heat exchanger", *Simulation Modelling Practice and Theory*, vol. 19, no. 2, pp. 777–784, 2011. DOI: 10.1016/j.simpat.2010.10.012.

[5] M. Abu-Khader, "Plate heat exchangers: Recent advances", *Renewable and Sustainable Energy Reviews*, vol. 16, no. 4, pp. 1883–1891, 2012. DOI: 10.1016/j.rser.2012.01.009.

[6] H. Qiao, V. Aute, H. Lee, K. Saleh, and R. Radermacher, "A new model for plate heat exchangers with generalized flow configurations and phase change", *International Journal of Refrigeration*, SI: New Developments in Boiling and Condensation, vol. 36, no. 2, pp. 622–632, Mar. 2013, ISSN: 0140-7007. DOI: 10.1016/j.ijrefrig.2012.11.020. [Online]. Available: http://www.sciencedirect.com/science/article/pii/S0140700712003283.

[7] J. Wolf, "Parallel flow recuperative multi-channel heat exchangers", *Arch. Bodowy Maszyn*, no. 9, Jan. 1962.

[8] ——, “General solution of the equations of parallelflow multichannel heat exchangers”, en, *International Journal of Heat and Mass Transfer*, vol. 7, no. 8, pp. 901–919, Aug. 1964, ISSN: 00179310. DOI: 10.1016/0017-9310(64)90146-2. [Online]. Available: http://linkinghub.elsevier.com/retrieve/pii/0017931064901462 (visited on 09/27/2018).

[9] T. Zaleski, “A general mathematical model of parallel-flow, multichannel heat exchangers and analysis of its properties”, en, *Chemical Engineering Science*, vol. 39, no. 7-8, pp. 1251–1260, 1984, ISSN: 00092509. DOI: 10.1016/0009-2509(84)85086-1. [Online]. Available: http://linkinghub.elsevier.com/retrieve/pii/0009250984850861 (visited on 09/27/2018).

[10] A. Settari and J. Venart, “Approximate method for the solution to the equations for parallel and mixed-flow multi-channel heat exchangers”, en, *International Journal of Heat and Mass Transfer*, vol. 15, no. 4, pp. 819–829, Apr. 1972, ISSN: 00179310. DOI: 10.1016/0017-9310(72)90123-8. [Online]. Available: http://linkinghub.elsevier.com/retrieve/pii/0017931072901238 (visited on 09/27/2018).

[11] T. Zaleski and K. Klepacka, “Approximate method of solving equations for plate heat exchangers”, en, *International Journal of Heat and Mass Transfer*, vol. 35, no. 5, pp. 1125–1130, May 1992, ISSN: 00179310. DOI: 10.1016/0017-9310(92)90173-P. [Online]. Available: http://linkinghub.elsevier.com/retrieve/pii/001793109290173P (visited on 09/27/2018).

[12] S. G. Kandlikar and R. K. Shah, “Multipass Plate Heat Exchangers—Effectiveness-NTU Results and Guidelines for Selecting Pass Arrangements”, en, *Journal of Heat Transfer*, vol. 111, no. 2, p. 300, 1989, ISSN: 00221481. DOI: 10.1115/1.3250678. [Online]. Available: http://HeatTransfer.asmedigitalcollection.asme.org/article.aspx?articleid=1440008 (visited on 09/27/2018).

[13] T. Zaleski and K. Klepacka, “Plate heat exchangers—method of calculation, charts and guidelines for selecting plate heat exchanger configurations”, en, *Chemical Engineering and Processing: Process Intensification*, vol. 31, no. 1, pp. 49–56, Apr. 1992, ISSN: 02552701. DOI: 10.1016/0255-2701(92)80008-Q. (visited on 09/25/2018).

[14] W. M. Kays and A. L. London, “Compact heat exchangers”, English, Jan. 1983. [Online]. Available: https://www.osti.gov/biblio/6132549 (visited on 10/08/2018).

[15] S.-Y. Wu, X.-F. Yuan, Y.-R. Li, and L. Xiao, “Exergy transfer effectiveness on heat exchanger for finite pressure drop”, *Energy*, vol. 32, no. 11, pp. 2110–2120, Nov. 1, 2007, ISSN: 0360-5442. DOI: 10.1016/j.energy.2007.04.010. [Online]. Available: http://www.sciencedirect.com/science/article/pii/S036054420700076X.

[16] M. Khairul, M. Alim, I. Mahbubul, R. Saidur, A. Hepbasli, and A. Hossain, “Heat transfer performance and exergy analyses of a corrugated plate heat exchanger using metal oxide nanofluids”, en, *International Communications in Heat and Mass Transfer*, vol. 50, pp. 8–14, Jan. 2014, ISSN: 07351933. DOI: 10.1016/j.icheatmasstransfer.2013.11.006.

[17] T. Wenterodt, C. Redecker, and H. Herwig, “Second law analysis for sustainable heat and energy transfer: The entropic potential concept”, *Applied Energy*, vol. 139, no. Supplement C, pp. 376–383, Feb. 2015, ISSN: 0306-2619. DOI: 10.1016/j.apenergy.2014.10.073. [Online]. Available: http://www.sciencedirect.com/science/article/pii/S0306261914011234.

[18] K. Nilpueng, T. Keawkamrop, H. S. Ahn, and S. Wongwises, “Effect of chevron angle and surface roughness on thermal performance of single-phase water flow inside a plate heat exchanger”, en, *International Communications in Heat and Mass Transfer*, vol. 91, pp. 201–209, Feb. 2018, ISSN: 07351933. DOI: 10.1016/j.icheatmasstransfer.2017.12.009. [Online]. Available: https://linkinghub.elsevier.com/retrieve/pii/S0735193317303263 (visited on 09/27/2018).

[19] Y. Zhang, C. Jiang, B. Shou, W. Zhou, Z. Zhang, S. Wang, and B. Bai, “A quantitative energy efficiency evaluation and grading of plate heat exchangers”, *Energy*, vol. 142, pp. 228–233, Supplement C Jan. 1, 2018, ISSN: 0360-5442. DOI: 10.1016/j.energy.2017.10.023. [Online]. Available: http://www.sciencedirect.com/science/article/pii/S0360544217316924.

[20] W. Q. Tan, L. Sun, Z. Jia, and J. Li, “Thermal-hydraulic Performance Analysis of Corrugated Plate Heat Exchanger”, en, *Chemical Engineering Transactions*, vol. 70, pp. 1153–1158, Aug. 2018, ISSN: 2283-9216. DOI: 10.3303/CET1870193. [Online]. Available:

https://www.cetjournal.it/index.php/cet/article/view/CET1870193 (visited on 09/27/2018).

[21] A. C. Caputo, P. M. Pelagagge, and P. Salini, "Heat exchanger optimized design compared with installed industrial solutions", *Applied Thermal Engineering*, vol. 87, pp. 371–380, Aug. 2015, ISSN: 1359-4311. DOI: 10.1016/j.applthermaleng.2015.05.010. [Online]. Available: http://www.sciencedirect.com/science/article/pii/S1359431115004524 (visited on 10/24/2018).

[22] V. Martinaitis and G. Streckiene, "Concerning exergy efficiency evaluation of heat recovery exchangers for air handling units", *International Journal of Exergy*, vol. 20, no. 3, pp. 381–404, Jan. 2016, ISSN: 1742-8297. DOI: 10.1504/IJEX.2016.077432. (visited on 06/08/2018).

[23] V. Martinaitis, J. Bielskus, K. Januševičius, and P. Bareika, "Exergy efficiency of a ventilation heat recovery exchanger at a variable reference temperature", en, *Mechanics*, vol. 23, no. 1, pp. 70–77, Mar. 2017, ISSN: 2029-6983. DOI: 10.5755/j01.mech.23.1.17678. (visited on 06/07/2018).

[24] D. Marmolejo and T. Gundersen, "A comparison of exergy efficiency definitions with focus on low temperature processes", *Energy*, vol. 44, pp. 447–489, Jul. 7, 2012. DOI: 10.1016/j.energy.2012.06.001.

[25] S. M. Baek, W. S. Seol, H. S. Lee, and J. I. Yoon, "Decreasing the Fouling of Heat Exchanger Plates Using Air Bubbles", in *Diffusion in Solids and Liquids V*, ser. Defect and Diffusion Forum, vol. 297, Trans Tech Publications, 2010, pp. 1199–1204. DOI: 10.4028/www.scientific.net/DDF.297-301.1199.

[26] A. Bani and J. Peschel, "Fouling in Plate Heat Exchangers: Some Practical Experience", en, in *Heat Exchangers - Basics Design Applications*, J. Mitrovic, Ed., InTech, Mar. 2012, ISBN: 978-953-51-0278-6. DOI: 10.5772/34026. [Online]. Available: http://www.intechopen.com/books/heat-exchangers-basics-design-applications/fouling-in-plate-heat-exchangers-some-practical-experience.

[27] S. D. Changani, M. T. Belmar-Beiny, and P. J. Fryer, "Engineering and chemical factors associated with fouling and cleaning in milk processing", *Experimental Thermal and Fluid Science*, vol. 14, no. 4, pp. 392–406, May 1997, ISSN: 0894-1777. DOI: 10.1016/S0894-1777(96)00141-0. [Online]. Available: http://www.sciencedirect.com/science/article/pii/S0894177796001410 (visited on 07/25/2018).

[28] K. R. Goode, K. Asteriadou, P. T. Robbins, and P. J. Fryer, "Fouling and Cleaning Studies in the Food and Beverage Industry Classified by Cleaning Type", en, *Comprehensive Reviews in Food Science and Food Safety*, vol. 12, no. 2, pp. 121–143, 2013, ISSN: 1541-4337. DOI: 10.1111/1541-4337.12000. [Online]. Available: https://onlinelibrary.wiley.com/doi/abs/10.1111/1541-4337.12000 (visited on 07/25/2018).

[29] C. Yaws, *Chemical Properties Handbook: Physical, Thermodynamics, Environmental Transport, Safety & Health Related Properties for Organic & Inorganic Chemical*, English, 1 edition. New York: McGraw-Hill Education, Oct. 1998, ISBN: 978-1-60623-527-0.

[30] U. Ascher, R. Mattheij, and R. Russell, *Numerical Solution of Boundary Value Problems for Ordinary Differential Equations*, ser. Classics in Applied Mathematics. Society for Industrial and Applied Mathematics, Jan. 1995, ISBN: 978-0-89871-354-1. DOI: 10.1137/1.9781611971231. [Online]. Available: https://epubs.siam.org/doi/book/10.1137/1.9781611971231 (visited on 07/25/2018).

[31] H. Martin, "A theoretical approach to predict the performance of chevron-type plate heat exchangers", *Chemical Engineering and Processing: Process Intensification*, vol. 35, no. 4, pp. 301–310, Jan. 1996, ISSN: 0255-2701. DOI: 10.1016/0255-2701(95)04129-X. [Online]. Available: http://www.sciencedirect.com/science/article/pii/025527019504129X (visited on 07/25/2018).

[32] T. M. Abou Elmaaty, A. E. Kabeel, and M. Mahgoub, "Corrugated plate heat exchanger review", *Renewable and Sustainable Energy Reviews*, vol. 70, no. Supplement C, pp. 852–860, Apr. 2017, ISSN: 1364-0321. DOI: 10.1016/j.rser.2016.11.266. [Online]. Available: http://www.sciencedirect.com/science/article/pii/S1364032116310516.

[33] R. Eldeeb, V. Aute, and R. Radermacher, "An Improved Approach for Modeling Plate Heat Exchangers Based on Successive Substitution in Alternating Flow Directions", *Inter-*

national Refrigeration and Air Conditioning Conference, Jan. 2016. [Online]. Available: http://docs.lib.purdue.edu/iracc/1684.

[34] A. Bejan, "General criterion for rating heat-exchanger performance", en, *International Journal of Heat and Mass Transfer*, vol. 21, no. 5, pp. 655–658, May 1978, ISSN: 00179310. DOI: 10.1016/0017-9310(78)90064-9. (visited on 10/10/2018).

[35] J. Guo, M. Xu, and L. Cheng, "The application of field synergy number in shell-and-tube heat exchanger optimization design", en, *Applied Energy*, vol. 86, no. 10, pp. 2079–2087, Oct. 2009, ISSN: 03062619. DOI: 10.1016/j.apenergy.2009.01.013. (visited on 10/10/2018).

[36] J. Guo, L. Cheng, and M. Xu, "Entransy dissipation number and its application to heat exchanger performance evaluation", en, *Science Bulletin*, vol. 54, no. 15, pp. 2708–2713, Aug. 2009, ISSN: 2095-9273, 2095-9281. DOI: 10.1007/s11434-009-0295-z. (visited on 10/10/2018).

[37] M. M. Kostic, "Entransy concept and controversies: A critical perspective within elusive thermal landscape", en, *International Journal of Heat and Mass Transfer*, vol. 115, pp. 340–346, Dec. 2017, ISSN: 00179310. DOI: 10.1016/j.ijheatmasstransfer.2017.07.059. (visited on 10/10/2018).

[38] A. Bejan, ""Entransy," and Its Lack of Content in Physics", en, *Journal of Heat Transfer*, vol. 136, no. 5, p. 055 501, Mar. 2014, ISSN: 0022-1481. DOI: 10.1115/1.4026527. (visited on 10/10/2018).

[39] D. P. Sekulic, E. Sciubba, and M. J. Moran, "Entransy: A misleading concept for the analysis and optimization of thermal systems", en, *Energy*, vol. 80, pp. 251–253, Feb. 2015, ISSN: 03605442. DOI: 10.1016/j.energy.2014.11.067. (visited on 10/10/2018).

[40] A. Bejan, G. Tsatsaronis, and M. Moran, *Thermal Design and Optimization*, 1 edition. New York: Wiley-Interscience, Nov. 28, 1995, 560 pp., ISBN: 978-0-471-58467-4.

[41] L. Perdomo-Hurtado, J. S. Rincón Tabares, D. Marmolejo Correa, and F. A. Perdomo, "Castor oil preheater selection based on entropy generation and exergy effectiveness criteria", *Energy*, vol. 120, pp. 805–815, Feb. 1, 2017, ISSN: 0360-5442. DOI: 10.1016/

j . energy . 2016 . 11 . 128. [Online]. Available: http : / / www . sciencedirect . com / science/article/pii/S0360544216317868 (visited on 02/22/2017).

[42] R. F. Barron, "Effect of Heat Transfer from Ambient on Cryogenic Heat Exchanger Performance", in *Advances in Cryogenic Engineering*, R. W. Fast, Ed., Boston, MA: Springer US, 1984, pp. 265–272, ISBN: 978-1-4613-9867-7 978-1-4613-9865-3. DOI: 10 . 1007 / 978-1-4613-9865-3_30.

4. GENERAL CONCLUSION

This research process has targeted the problem of heat exchanger evaluation applying methodologies of "Thermal design and optimization" as second law analysis. This project impacts directly on industrial energy use because those equipment are fundamental on every place where energy has to be shifted between media (e.g. food and beverage processing, pharmaceutical, rubber and petrochemical industries, biofuel production and power plants).

The problem was solved developing a methodology based on Second Law of Thermodynamics indexes to rate feasible heat exchangers. This methodology can be used in a particular situation, as in chapter 2, or in a wider context with the correct assumptions, as saw in chapter 3. This was possible this was possible thanks to the developed algorithms (represented on Figs. **2-1**, **2-6** and **3-1**) that couple heat exchanger thermodynamic models with entropy and exergy indicators.

Chapter 2 explained how to select a heat exchanger based on rigorous design model and a Second Law evaluation for a particular situation. According to obtained charts (Fig. **2-7** and Fig. **2-8**) there is an energy optimum that is reached on manufacturable heat exchanger. The main contribution is that empirical based recommendation for designing established by Tubular Heat Exchanger Manufacturer Association on Shell-&-Tube are in a very good agreement with second law performance on equipment.

This methodology can be used for selecting heat exchanger type in any situation where fluid thermo-physical properties data and process operation data are available. Additionally, if there is a geometry based formulation to rate /design the selected type of heat exchanger, a specific equipment could be compared to anther based on accessible raw materials and components.

On the other hand, in chapter 3 a wider approach was developed, to generate a set of feasible equipment that can be a guide for many liquid-liquid gasketed-plate situations because water is used as both working fluid. In this case, an installation variable (cold fluid port connection allocation) and room temperature were taken into account. Those variables are always present when a gasketed-plate heat exchanger solution is needed and cannot be skipped for industries designer and engineers. According to this, low temperature processes are those that degrades energy the most because they expel higher amounts of entropy to surroundings than those that work above room temperature. This fact can be an advantage or disadvantage taking in account the heat transfer process aim. In addition, heat exchanger fluids connection ports allocation should be at same height and in opposite sides of the heat exchanger, whenever possible, to ensure the lowest waste and the best energy use.

It is to highlight that all obtained useful design charts compares NTU (Eq.3-8) with ε (Eq.3-7), ε_e (Eq. 3-11), S^* (Eqs. 3-9 and 3-10), N_{EPL} (Eq. 3-13), that are non-dimensional functions. The above situation yields in simulation results independence from particular situations as heat exchanger geometric values or fluid selection, among others.

4.1. Recomendations and Future Work

To supplement methodologies presented in this work, researchers and engineers can face it from two main topics thermo-economics and phase-change. Based on those topics, some future work can be conducted on this field:

- It is known that good designs are reached when all available resources are used in an optimal way. On the current approach, energy use may be near an optimum and it could be reached by setting an energy efficiency function as an objective function in an optimization algorithm. Nevertheless, "Thermal design and optimization" also includes the economic path. This restriction has been omitted, but it is very important to generate feasible configurations. It is recommended that second law analysis come along with an economic analysis due to best energy performance have high monetary cost. Since thermo-economics is a better approach to evaluate the equipment selection than only energy efficiency or only

minimum cost, the exposed methodology is suitable to be part of an MINLP optimization perspective. Therefore, it has to include rigorous thermo-economic model. Traditionally, a cost function for a heat exchanger is heat transfer area based and corrected by some parameters. However, to continue with the same strategy on this dissertation, it is necessary that capital cost be coupled with material quantity, price, its manufacturing operations and the geometry.

- A specific situation have been solve for liquid-liquid heat exchangers, where thermo-physical properties depend mainly on temperature. However, gas and vapor phase heat exchanger were omitted because they need both temperature and pressure to establish their thermo-physical properties. As a consequence, thermodynamic models used on this approach must be changed to other that can generate temperature and pressure profiles inside the heat exchanger. Additionally if there is multiphase flow inside the equipment, a third independent property is needed and the heat transfer mechanism variates with it, that yields in situation where researchers and engineers are limited by the availability of phase change correlations for the working fluids.

Finally, the methodologies exposed in chapters 2 and 3 could be used to select equipment different from heat exchangers. It depends on the availability of rigorous design models for the equipment and indicators based on the second law of thermodynamics that represent the phenomenon occurring within the equipment.